AWARD NUMBER: W81XWH-17-1-0404

TITLE: Investigating the Molecular Mechanisms of Acquired Resistance to BET Bromodomain Inhibitors in Castration-Resistant Prostate Cancer

PRINCIPAL INVESTIGATOR: Dr. Irfan Asangani

CONTRACTING ORGANIZATION: Trustees of the University of Pennsylvania
Philadelphia, PA 19104

REPORT DATE: Sep 2018

TYPE OF REPORT: Annual

PREPARED FOR: U.S. Army Medical Research and Materiel Command
Fort Detrick, Maryland 21702-5012

REPORT DOCUMENTATION PAGE

Form Approved
OMB No. 0704-0188

1. REPORT DATE	2. REPORT TYPE	3. DATES COVERED
Sept 2018	Annual	1 Sep 2017 - 31- Aug 2018

4. TITLE AND SUBTITLE

Investigating the Molecular Mechanisms of Acquired Resistance to BET Bromodomain Inhibitors in Castration-Resistant Prostate Cancer

5a. CONTRACT NUMBER

5b. GRANT NUMBER
W81XWH-17-1-0404

5c. PROGRAM ELEMENT NUMBER

6. AUTHOR(S)
Irfan Asangani

E-Mail:asangani@pennmedicine.upenn.edu

5d. PROJECT NUMBER

5e. TASK NUMBER

5f. WORK UNIT NUMBER

7. PERFORMING ORGANIZATION NAME(S) AND ADDRESS(ES)

Trustees of the University of Pennsylvania
3451 Walnut St,
Philadelphia, PA 19104

8. PERFORMING ORGANIZATION REPORT NUMBER

9. SPONSORING / MONITORING AGENCY NAME(S) AND ADDRESS(ES)

U.S. Army Medical Research and Materiel Command
Fort Detrick, Maryland 21702-5012

10. SPONSOR/MONITOR'S ACRONYM(S)

11. SPONSOR/MONITOR'S REPORT NUMBER(S)

12. DISTRIBUTION / AVAILABILITY STATEMENT

Approved for Public Release; Distribution Unlimited

13. SUPPLEMENTARY NOTES

14. ABSTRACT

BRD4 plays a major role in the transcription networks orchestrated by androgen receptor (AR) in castration resistant prostate cancer (CRPC). Several BET inhibitors (BETi) that displace BRD4 from chromatin are being evaluated in clinical trials for CRPC. Here we describe mechanisms of acquired resistance to BETi that are amenable to targeted therapies in CRPC. BETi-resistant CRPC cells displayed cross-resistance to a variety of BETi in the absence of gatekeeper mutations, exhibited reduced chromatin-bound BRD4, and were less sensitive to BRD4 degraders/knockdown, suggesting a BRD4-independent transcription program. Transcriptomic analysis revealed reactivation of AR-signaling due to CDK9-mediated phosphorylation of AR, resulting in sensitivity to CDK9 inhibitors and enzalutamide. Additionally, increased DNA damage associated with PRC2-mediated transcriptional silencing of DDR genes was observed leading to PARP inhibitor sensitivity. Collectively, our results identify the therapeutic limitation of BETi as a monotherapy, however; our BETi-resistant data suggests unique opportunities for combination therapies in treating CRPC.

15. SUBJECT TERMS
CRPC, Chromatin readers, BRD4, AR, BET bromodomain inhibitors, Transcriptional plasticity, PROTAC, Synthetic lethal, CDK9, PARP, DNA damage, Olaparib, PRC2 complex, EZH2.

16. SECURITY CLASSIFICATION OF:			17. LIMITATION OF ABSTRACT	18. NUMBER OF PAGES	19a. NAME OF RESPONSIBLE PERSON
a. REPORT	b. ABSTRACT	c. THIS PAGE			USAMRMC
Unclassified	Unclassified	Unclassified	Unclassified		19b. TELEPHONE NUMBER *(include area code)*

Table of Contents

Page

1. **INTRODUCTION:** *Narrative that briefly (one paragraph) describes the subject, purpose and scope of the research.*

   There is a critical need to better understand the mechanism of acquired resistance to targeted therapies in castration resistant prostate cancer. Our proposal represents the first step towards understanding the mechanism of acquired resistance to BET inhibitors that has shown immense promise in preclinical cancer models and early results from clinical trials have also been encouraging with durable patient responses in CRPC patients. This proposed work has important translational relevance and high potential clinical impact. The underlying hypothesis of this proposal is that resistance to BET inhibitor therapy leads to reactivation of AR signaling pathway due to widespread re-orchestration of the chromatin landscape; however with increased DNA damage and modulated PRC2 activity, BETi resistant cells are sensitive to anti-androgens, PARP inhibitors and EZH2 inhibitors.

2. **KEYWORDS:** CRPC, Chromatin readers, BRD4, AR, BET bromodomain inhibitors, Transcriptional plasticity, PROTAC, Synthetic lethal, CDK9, PARP, DNA damage, Olaparib, PRC2 complex, EZH2.

3. **ACCOMPLISHMENTS:** *The PI is reminded that the recipient organization is required to obtain prior written approval from the awarding agency Grants Officer whenever there are significant changes in the project or its direction.*

   - **What were the major goals of the project?** *List the major goals of the project as stated in the approved SOW. If the application listed milestones/target dates for important activities or phases of the project identify these dates and show actual completion dates or the percentage of completion.*

   - **Specific Aim 1: To elucidate the mechanism of transcriptional plasticity causing acquired resistance to BETi therapy by integrative genomic, epigenomic and transcriptomic profiling.**

   - Task 1: To investigate genomic alteration in BETi resistant cells (25% completed)

   - Task 2: To investigate changes in the chromatin landscape (15% completed)

   - Task 3: To investigate enhancer deregulation and its effect on AR chromatin recruitment in BETi resistant cells (50% completed)

   - **Specific Aim 2: To elucidate the mechanism of AR signaling reactivation and the role of PRC2 in acquired resistant to BETi and to screen for novel epigenetic regulators of a BETi resistant state.**

   - Task 1: To investigate the role of PARP in the activation of AR signaling pathway in prostate cancer cells with acquired resistance to BETi (50% completed).

   - Task 2: To elucidate the role of PRC2 in acquired resistance to BETi in prostate cancer cells (35% completed).

   - Task 3: To identify novel epigenetic and transcriptional mediators that alleviate BET inhibitor resistance. (5% completed).

   - **Specific Aim 3: To evaluate BETi drug combinations focusing on Enzalutamide/PARPi/EHZ2i combinations in vivo.**

   - Task 1: Mouse xenograft therapeutic studies with BETi sensitive and acquired resistant prostate cancer models. (will be initiated in the next 2-3 months)

- Task 2: To utilize physiologically relevant prostate cancer models to test enzalutamide/PARPi/EZH2i with BET inhibitor therapy. (will be initiated in the next 6 months).

- **What was accomplished under these goals?**
  - Significant majority of the goals were achieved that resulted in the high impact publication titled "*Resistance to BET Inhibitor Leads to Alternative Therapeutic Vulnerabilities in Castration-Resistant Prostate Cancer"* in the journal **Cell Reports**. For complete description of the data and conclusion, please refer to the published manuscript attached.

- **What opportunities for training and professional development has the project provided?**
  - Participated and presented a poster in the AACR annual meeting 2018 held in Chicago.

- **How were the results disseminated to communities of interest?**
  - *"Nothing to Report."*

- **What do you plan to do during the next reporting period to accomplish the goals?**
  - Continue to accomplish more on the proposed aims to understand the BETi resistance in CRPC by performing more detailed molecular biology experiments, NGS assays and in vivo xenograft experiments.

4. **IMPACT:** *Describe distinctive contributions, major accomplishments, innovations, successes, or any change in practice or behavior that has come about as a result of the project relative to:*

   - **What was the impact on the development of the principal discipline(s) of the project?**
     - We hope that the published results as a manuscript in the journal "Cell Reports" will help in the rationale design of a combination therapy for refractory castration resistant prostate cancer patients. Further, the results described will help us appreciate the diverse cellular pathways a cancer cell takes to overcome the BET inhibitor action.

   - **What was the impact on other disciplines?**
     - Our published results will help explain the BET inhibitors resistance in diverse cancer type including BRD4 dependent cancers such as cancer of breast, thyroid, sarcoma etc.

   - **What was the impact on technology transfer?**
     - Nothing to Report.

   - **What was the impact on society beyond science and technology?**
     - Nothing to Report.

5. **CHANGES/PROBLEMS:** "Nothing to Report,"

6. **PRODUCTS:** *List any products resulting from the project during the reporting period. If there is nothing to report under a particular item, state "Nothing to Report."*

   - **Publications, conference papers, and presentations**
     Report only the major publication(s) resulting from the work under this award.

- **Journal publications.**
- Journal: Cell Reports (published in February 2018)

  Title: Resistance to BET Inhibitor Leads to Alternative Therapeutic Vulnerabilities in Castration-Resistant Prostate Cancer
- Authors: Pawar A, Gollavilli PN, Wang S, Asangani IA.
- https://www.sciencedirect.com/science/article/pii/S2211124718301797?via%3Dihub
- Acknowledgement of federal support: YES
- **Other publications, conference papers, and presentations.**
- AACR Annual Meeting 2018.
- Abstract 1394: Resistance to BET inhibitor leads to new therapeutic vulnerabilities in castration resistant prostate cancer
- Authors: Pawar A, Asangani IA.

- **Website(s) or other Internet site(s)**
  Nothing to report
- **Technologies or techniques**
  Nothing to report
- **Inventions, patent applications, and/or licenses**
  Nothing to report
- **Other Products**
  Identify any other reportable outcomes that were developed under this project. Reportable outcomes are defined as a research result that is or relates to a product, scientific advance, or research tool that makes a meaningful contribution toward the understanding, prevention, diagnosis, prognosis, treatment, and/or rehabilitation of a disease, injury or condition, or to improve the quality of life. Examples include:
  - *research material : BET inhibitor resistant LNCaP and 22RV1 prostate cancer cells have been developed. We are open to share those lines to any interested researcher upon request.*

7. **PARTICIPANTS & OTHER COLLABORATING ORGANIZATIONS**

- **What individuals have worked on the project?**
  - *Provide the following information for: (1) PDs/PIs; and (2) each person who has worked at least one person month per year on the project during the reporting period, regardless of the source of compensation (a person month equals approximately 160 hours of effort). If information is unchanged from a previous submission, provide the name only and indicate "no change."*

Name:	Irfan Asangani
Project Role:	Principal Investigator
Researcher Identifier (e.g. ORCID ID):	
Nearest person month worked:	2
Contribution to Project:	Dr. Asangani continues to supervise the study
Funding Support:	Zenith Epigenetics, DOD

Name:	Qu Deng
Project Role:	Post Doctoral Researcher
Researcher Identifier (e.g. ORCID ID):	
Nearest person month worked:	6
Contribution to Project:	Dr. Deng has performed work related to development and characterization of BETi resistant prostate cancer cells.
Funding Support:	DOD, Institutional Funding

- **Has there been a change in the active other support of the PD/PI(s) or senior/key personnel since the last reporting period?**

  Dr. Asangani's K99/R00 ended on 8/31/18 (7.2 CM) and effort has increased on SRA with Zenith Epigenetics (1.2CM to 7.2CM) and on this award (2.4CM to 3.6CM).

- **What other organizations were involved as partners?**

  - *Nothing to Report.*

8. **SPECIAL REPORTING REQUIREMENTS**

   - **COLLABORATIVE AWARDS:** *For collaborative awards, independent reports are required from **BOTH** the Initiating PI and the Collaborating/Partnering PI. A duplicative report is acceptable; however, tasks shall be clearly marked with the responsible PI and research site. A report shall be submitted to https://ers.amedd.army.mil for each unique award.*

   - **QUAD CHARTS:** *If applicable, the Quad Chart (available on https://www.usamraa.army.mil) should be updated and submitted with attachments.*

9. **APPENDICES:** *Attach all appendices that contain information that supplements, clarifies or supports the text. Examples include original copies of journal articles, reprints of manuscripts and abstracts, a curriculum vitae, patent applications, study questionnaires, and surveys, etc. Reminder: Pages shall be consecutively numbered throughout the report. **DO NOT RENUMBER PAGES IN THE APPENDICES.***

Cell Reports

Report

Resistance to BET Inhibitor Leads to Alternative Therapeutic Vulnerabilities in Castration-Resistant Prostate Cancer

Graphical Abstract

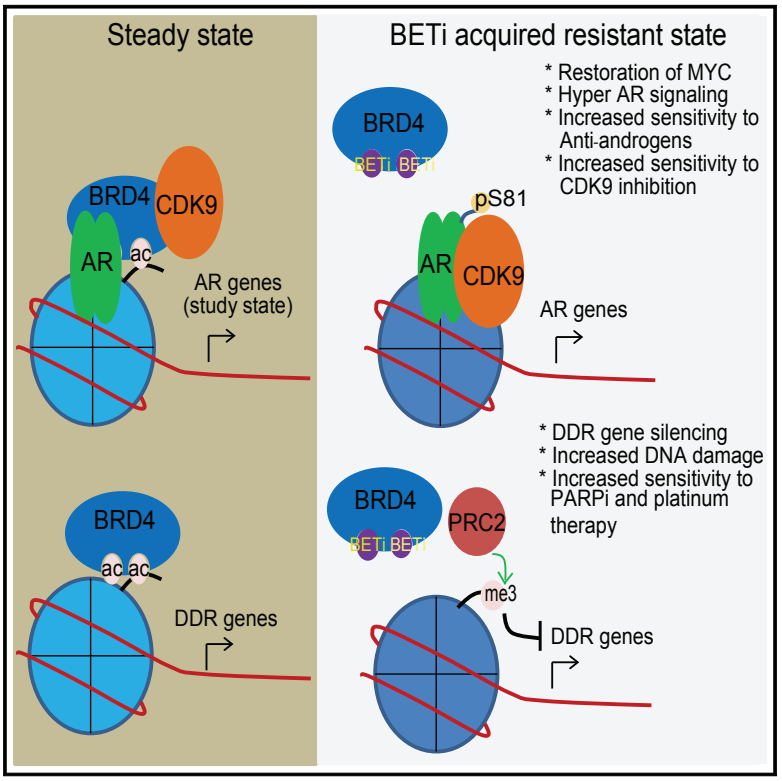

Highlights

- BET-inhibitor-resistant prostate cancer cells display BRD4-independent transcription
- Reactivation of AR signaling due to CDK9-mediated phosphorylation of AR
- BET-inhibitor-resistant cells display increased sensitivity to CDK9 and AR blockade
- PRC2-mediated silencing of DDR genes causes sensitivity to PARPi in the resistant cells

Authors

Aishwarya Pawar, Paradesi Naidu Gollavilli, Shaomeng Wang, Irfan A. Asangani

Correspondence

asangani@upenn.edu

In Brief

Resistance to targeted therapies is a major problem. Pawar et al. investigate the potential mechanisms of acquired resistance to BET inhibitors in prostate cancer and identify actionable targets to overcome the resistance. This study highlights the therapeutic limitation of BET inhibitors as a monotherapy and suggests potential combination therapies in treating prostate cancer.

Data and Software Availability

GSE103082

Pawar et al., 2018, Cell Reports 22, 2236–2245
February 27, 2018
https://doi.org/10.1016/j.celrep.2018.02.011

CellPress

OPEN ACCESS
CellPress

Cell Reports
Report

Resistance to BET Inhibitor Leads to Alternative Therapeutic Vulnerabilities in Castration-Resistant Prostate Cancer

Aishwarya Pawar,[1] Paradesi Naidu Gollavilli,[1] Shaomeng Wang,[2] and Irfan A. Asangani[1,3,4,*]
[1]Department of Cancer Biology, Perelman School of Medicine, University of Pennsylvania, Philadelphia, PA, USA
[2]Departments of Internal Medicine, Pharmacology, and Medicinal Chemistry, University of Michigan, Ann Arbor, MI, USA
[3]Department of Cancer Biology, Abramson Family Cancer Research Institute, Epigenetics Institute, Perelman School of Medicine, University of Pennsylvania, 421 Curie Boulevard, BRBII/III, Philadelphia, PA 19104, USA
[4]Lead Contact
*Correspondence: asangani@upenn.edu
https://doi.org/10.1016/j.celrep.2018.02.011

SUMMARY

BRD4 plays a major role in the transcription networks orchestrated by androgen receptor (AR) in castration-resistant prostate cancer (CRPC). Several BET inhibitors (BETi) that displace BRD4 from chromatin are being evaluated in clinical trials for CRPC. Here, we describe mechanisms of acquired resistance to BETi that are amenable to targeted therapies in CRPC. BETi-resistant CRPC cells displayed cross-resistance to a variety of BETi in the absence of gatekeeper mutations, exhibited reduced chromatin-bound BRD4, and were less sensitive to BRD4 degraders/knockdown, suggesting a BRD4-independent transcription program. Transcriptomic analysis revealed reactivation of AR signaling due to CDK9-mediated phosphorylation of AR, resulting in sensitivity to CDK9 inhibitors and enzalutamide. Additionally, increased DNA damage associated with PRC2-mediated transcriptional silencing of DDR genes was observed, leading to PARP inhibitor sensitivity. Collectively, our results identify the therapeutic limitation of BETi as a monotherapy; however, our BETi resistance data suggest unique opportunities for combination therapies in treating CRPC.

INTRODUCTION

The potential of targeting bromodomain and extraterminal domain (BET) proteins in cancer has fueled the development of a variety of BET inhibitors (BETi) in several malignancies, including metastatic castration-resistant prostate cancer (CRPC). BET proteins are an important class of chromatin readers involved in transcriptional control and consist of BRD2, -3, and -4, as well as BRDT (Belkina and Denis, 2012). BETi that target the amino-terminal acetyl reader bromodomains of BRD2/3/4 exhibit anti-proliferative effects in many different types of malignancies (Delmore et al., 2011; Lockwood et al., 2012). Recently, we showed that AR (androgen receptor)-signaling-competent human CRPC cells are preferentially sensitive to BET inhibition (Asangani et al., 2014). In contrast to the anti-androgen, enzalutamide, the BETi functions downstream of AR and potently abrogates BRD4 localization to AR target loci and AR-mediated gene transcription, including *TMPRSS2-ERG* fusion and its oncogenic activity. Combination treatment of enzalutamide or ARN509 with BETi led to even greater inhibition of prostate tumor growth than anti-androgen alone (Asangani et al., 2016). Preclinical data from a number of studies, including ours, demonstrated the BETi as a promising drug for CRPC (Chan et al., 2015; Raina et al., 2016; Wyce et al., 2013), and currently, multiple BET inhibitors are undergoing clinical testing (https://clinicaltrials.gov). Although, early results from BETi clinical trials have been encouraging, with durable responses in hematological malignancies, lessons from other targeted cancer therapies, such as enzalutamide and abiraterone, suggest that acquired resistance will limit responsiveness to BETi treatment in CRPC (Antonarakis et al., 2014). Therefore, the evaluation of resistance mechanisms is crucial in optimizing the clinical efficacy of these epigenetic drugs.

Using preclinical models, a number of groups have reported pleiotropic mechanisms of resistance to BETi, including compensatory β-catenin activation in leukemia, kinome-reprogramming in ovarian cancer, and BRD4 conformational changes in triple-negative breast cancer (Fong et al., 2015; Kurimchak et al., 2016; Rathert et al., 2015; Shu et al., 2016). These data imply that mechanisms underlying acquired BETi resistance are tumor type specific. Therefore, identification of molecular mechanisms leading to acquired BETi resistance may suggest specific therapeutic strategies for resensitizing prostate cancer (PCa) cells to BETi and allow the design of rationale combination therapies in treating CRPC.

In this study, we demonstrate that acquired resistance to BETi in CRPC cells is due to the loss of BRD4 chromatin binding, leading to reactivation of AR signaling by CDK9. Reduced BRD4 from the chromatin due to continued blockade of its BET domains by BETi also resulted in PRC2-mediated transcriptional silencing of DNA damage response (DDR) genes, ensuing increased DNA damage in the BETi-resistant cells that become sensitive to PARP inhibitors and cisplatin.

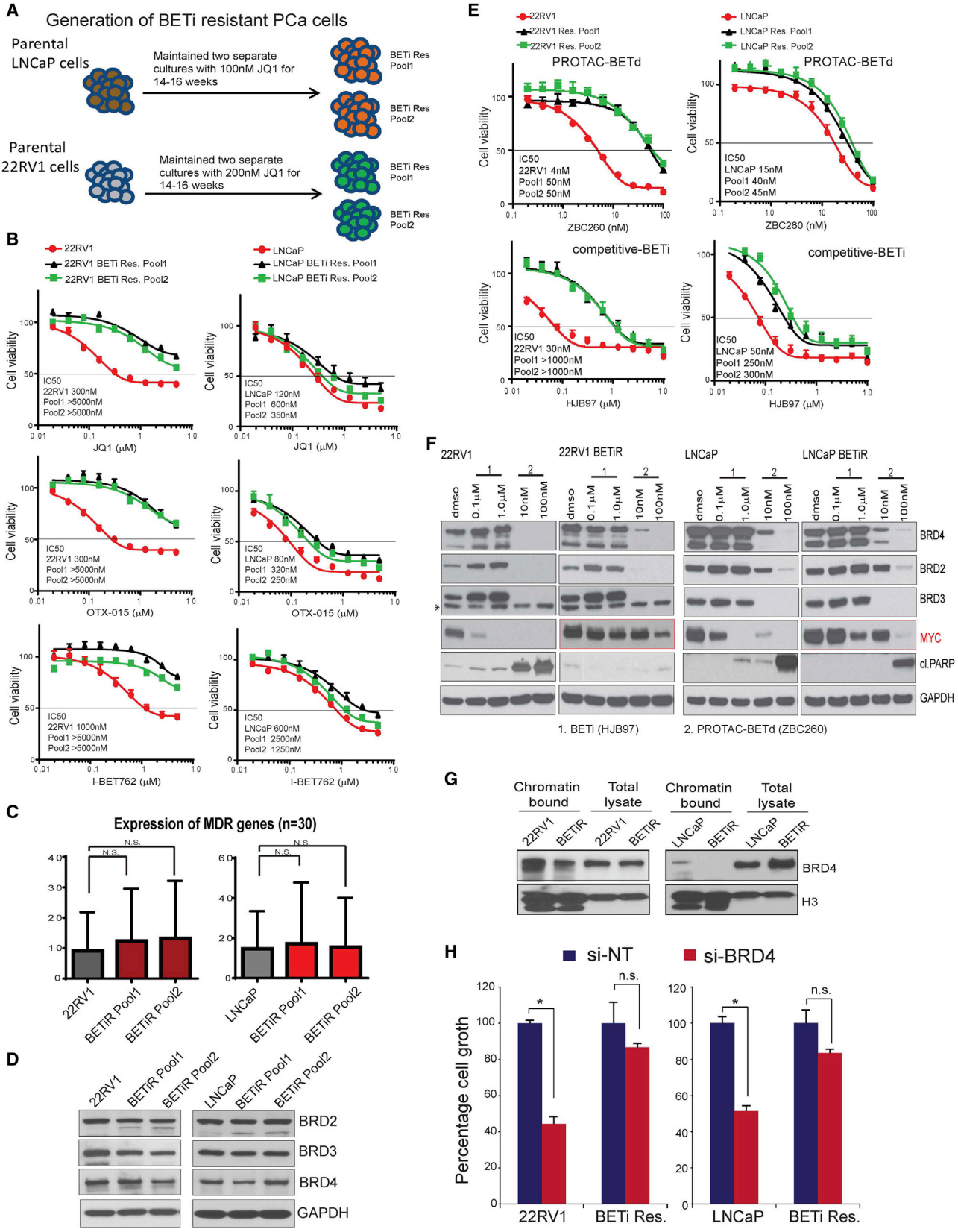

(legend on next page)

RESULTS AND DISCUSSION

BRD4 Is Dispensable in BET-Inhibitor-Resistant PCa Cells

To investigate the mechanism of acquired resistance to BET inhibitors in PCa cells, we cultured two AR-positive, BET-inhibitor-sensitive PCa cell lines, LNCaP and 22Rv1 (Asangani et al., 2014), with JQ1 for an extended period, establishing two independent clones of JQ1-resistant lines (BETi-resistant cells) (Figure 1A). Though the parental LNCaP and 22Rv1 cells were exquisitely sensitive to JQ1, the gIC_{50} for JQ1 were 3- to 10-fold higher in both the derived resistant lines (Figure 1B). Interestingly, JQ1-resistant subclones also showed a similar level of resistance to the chemically distinct BET inhibitors, OTX-015 and I-BET762 (Figure 1B), currently in phase I clinical trials for CRPC (https://clinicaltrials.gov). RNA-sequencing (RNA-seq) analysis of the BETi-resistant cells did not show any apparent increase in the expression of multi-drug resistance (MDR) ABC transporter genes, ruling out the possibility of a generic drug resistance mechanism arising from the activation of drug pumps (Figure 1C). Loss of sensitivity to BET inhibitors in the resistant lines was also not a consequence of changes in the levels of BRD2/3/4 proteins, as no significant difference was observed in the expression of BRD2, BRD3, or BRD4 in BETi-resistant cells (Figures 1D and S1C). Moreover, analysis of the sequence reads from the RNA-seq data did not reveal mutations in the BRD2/3/4 (data not shown) or any significant change in their transcripts (Figures S1A and S1B). Interestingly, cellular thermal shift assay (CETSA) analysis showed that JQ1 was still engaging with BRD4 in the resistant cells, ruling out the possibility of lack of target engagement by the BETi (Figure S1D). These observations prompted us to test whether BRD4 is essential in the BETi-resistant cells and whether degradation of the BRD4 will restore BETi sensitivity. Treating cells with proteolysis targeting chimera (PROTAC) BET degrader ZBC260 (Zhou et al., 2017) demonstrated a 3- to 10-fold higher gIC_{50} in the resistant lines, similar to that of other tested BET inhibitors, including the HJB97, a control BETi for ZBC260 lacking the thalidomide linker (Figure 1E). However, ZBC260 completely degraded BRD4 as well as BRD2/3 proteins in both parental and BETi-resistant lines (Figure 1F). Unlike the BETi-resistant cells, apoptosis (cleaved PARP) was evident in the parental lines after treatment with the competitive and BET degrader compound (Figure 1F). Intriguingly, MYC, which is an important target of BET proteins, was restored and was not significantly affected by HJB97 or ZBC260 in the resistant cells, despite degradation of BRD4, implicating transcriptional plasticity in the BETi-acquired resistant state that is independent of BRD4 function (Figure 1F; Figures S1E–S1H). Interestingly, knockdown of MYC in the BETi-resistant cells resulted in decreased proliferation, which was equivalent to that in parental controls, suggesting that its restoration, in part, drives the proliferation of BETi-resistant cells (Figures S1I and S1J). These data suggest that persistent blockade by BETi in resistant cells may prevent BRD4 binding to chromatin through its BET domain. As expected, we found significantly less chromatin-bound BRD4 in the resistant cells in comparison to the parental cells (Figure 1G). Furthermore, unlike parental cells, the BETi-resistant derivatives were not sensitive to BRD4 knockdown, which coincided with the lack of MYC downregulation (Figure 1H; Figures S1K and S1L). Together, these data strongly suggest that acquired resistance to BET inhibitors in PCa cells is due to the activation of cellular pathways independent of BRD4's chromatin function.

CDK9 Mediated Reactivation of AR Signaling in the BETi-Resistant PCa Cells

To investigate the cellular pathways responsible for the BETi-acquired resistant state, we analyzed the transcriptomes of the sensitive and resistant cells (Table S1). RNA-seq data showed differential expression of 1,450 genes in BETi-resistant LNCaP derivatives, whereas 2,099 genes were differentially expressed in BETi-resistant 22Rv1 derivatives (Figure S2A). A total of 512 genes were common to both the BETi-resistant lines, implying alterations of similar pathways (Figure S2B). Interestingly, many of the genes that were modulated in the resistant lines were either targets of AR, involved in the DDR, or related to apoptosis. AR is a major driver in metastatic castration-resistant prostate cancer (mCRPC) (Chen et al., 2004; Robinson et al., 2015), and most prostate tumors continue to rely on AR signaling. Progression to CRPC after androgen ablation therapy is predominantly driven by deregulated AR signaling. Reactivation of AR signaling by means of an AR amplification/overexpression/mutation/splice variant is a known mechanism of resistance to anti-androgens or androgen deprivation therapy in PCa cells (Watson et al., 2015). We explored whether the reactivation of AR signaling is a driver of acquired resistance to BETi in our models. Gene set enrichment analysis (GSEA) revealed a significant positive enrichment of AR target genes in both BETi-resistant LNCaP (Figure 2A). Multiple canonical AR target genes were found to be overexpressed in BETi-resistant LNCaP cells, and some of these were also overexpressed in BETi-resistant 22Rv1 cells as determined by qRT-PCR (Figure S2C). Interestingly, the AR transcript levels were not increased in the BETi-resistant cells (Figure S2C). KLK3/prostate-specific antigen

Figure 1. BRD4 Is Dispensable in BET-Inhibitor-Resistant PCa Cells

(A) Schematic depicting the strategy used to develop BETi (JQ1)-resistant PCa cells.

(B) Representative dose-response curves for the parental and BETi-resistant cells treated with JQ1, OTX-015, and I-BET762. n = 4 wells of a 96-well plate per condition. Half-maximum inhibitory concentration (IC_{50}) is shown.

(C) The expression of 30 ABC transporters was analyzed by RNA-seq. N.S., not significant.

(D) Immunoblot analysis of BRD2/3/4 protein levels in the indicated cells. GAPDH was used as internal control.

(E) Representative dose-response curves for cells treated with BET inhibitor (HJB97) and compound 23 PROTAC-BET degrader (ZBC260).

(F) Immunoblot for BRD2, BRD3, BRD4, MYC, cleaved PARP, and GAPDH after 24-hr drug treatment in indicated cells. Asterisk indicates a non-specific band.

(G) Decreased chromatin-bound BRD4 in BETi-resistant cells. Immunoblot for BRD4 in chromatin and total protein fractions.

(H) Cell proliferation upon BRD4 knockdown. Data indicate mean ± SD. *$p < 0.05$, by two-tailed Student's t test. n.s., not significant.

See also Figure S1.

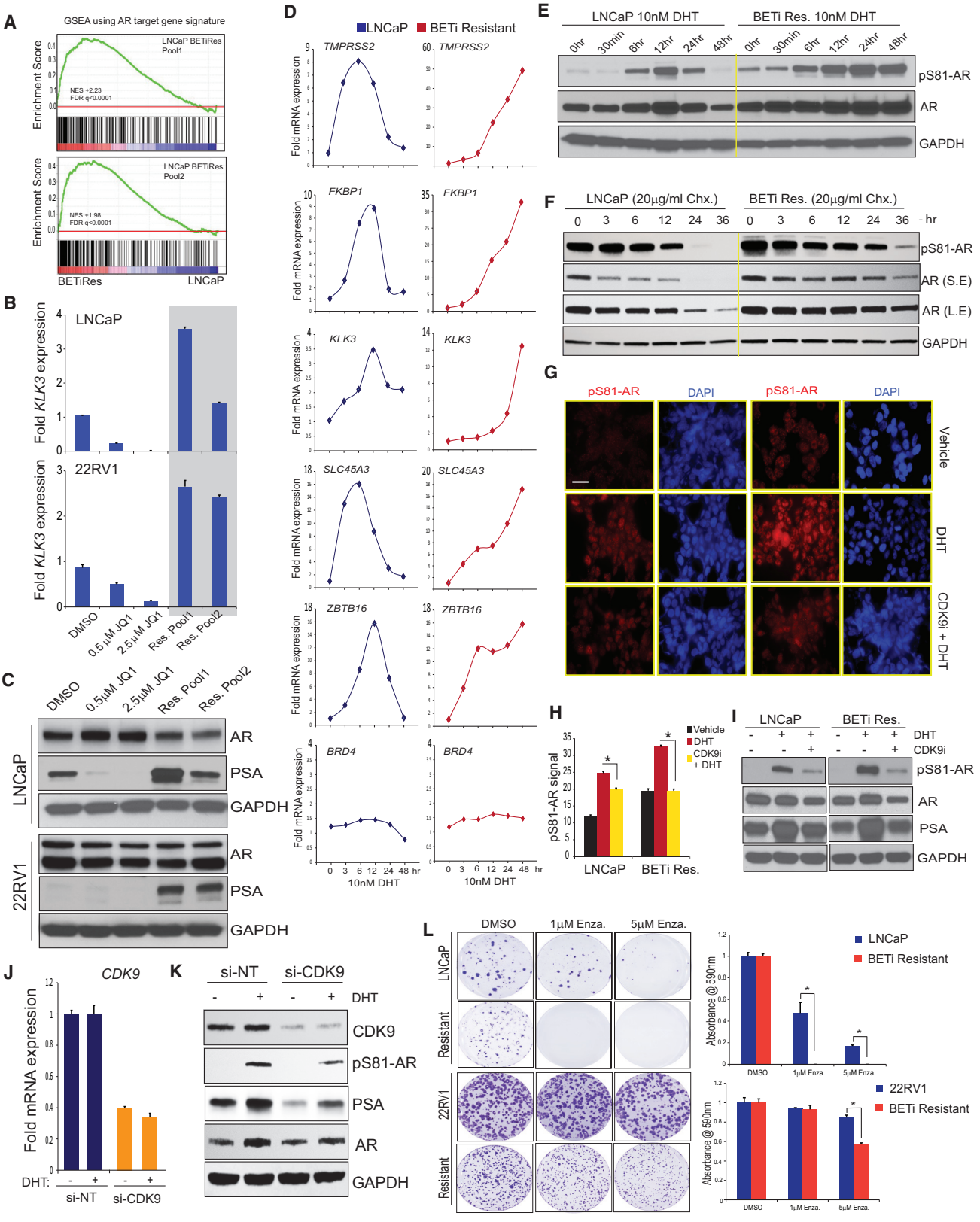

(legend on next page)

(PSA) was expressed at high levels in BETi-resistant cells, though the AR protein levels were not increased, and as expected, transient treatment with BETi led to the loss of PSA expression in the parental cells (Figures 2B and 2C). Moreover, drug withdrawal in the BETi-resistant cells led to only partial reversal of AR target genes (Figure S2D). To investigate the mechanism of hyper-activated AR signaling in the absence of increased AR expression in the BETi-resistant cells, we performed qRT-PCR for multiple AR target genes in the cells treated with androgen (dihydrotestosterone [DHT]) for different time points after 3 days of hormone deprivation. As expected, the AR target genes were induced by DHT stimulation by 3 hr, reaching the peak at 6–12 hr, and returned to pre-stimulation levels by 48 hr in the LNCaP cells. However, the fold induction of the same genes was significantly higher in the BETi-resistant cells, and the expression levels were continually increasing, even at 48 hr, strongly suggesting a hyper-activated AR transcriptional output (Figure 2D). This was matched by persistently increased phosphorylated S81-AR, a known regulator of AR transcriptional activity (Gordon et al., 2010), in the BETi-resistant cells compared to parental controls (Figures 2E, S2E, and S2F). Furthermore, in comparison to parental LNCaP, pS81-AR and total AR were more stable in the BETi-resistant cells, suggesting that the observed increase in the AR stability could be due to its increased phosphorylation or other post-translational modifications (Figures 2F and S2F). CDK9 phosphorylates S81 on AR and stabilizes its chromatin binding for transcription (Chen et al., 2012). CDK9 is the catalytic subunit of the Positive Transcription Elongation Factor b (p-TEFb) complex that associates with the BRD4 protein and phosphorylates the C-terminal domain (CTD) of RNAPII for productive transcription elongation (Lu et al., 2015). To determine the contribution of CDK9 toward AR hyperactivity in resistant cells, we treated them with LDC000067, a CDK9-specific inhibitor, and found significant inhibition of DHT-induced phosphorylation of S81-AR and its transcriptional activity in BETi-resistant LNCaP cells as compared to controls (Figures 2G–2I and S3A). Similar results were obtained in BETi-resistant cells grown in normal media (Figure S3B). In addition, in a cell viability assay, BETi-resistant cells displayed sensitivity to LDC000069 and dinaciclib, a clinical grade CDK9 inhibitor, suggesting an increased dependency on CDK9 activity (Figure S3C). Importantly, knockdown of CDK9 led to decreased phosphorylation of S81-AR, with a concomitant decrease in AR target gene expression in the BETi-resistant cells (Figures 2J and 2K). Furthermore, CDK9 knockdown had significantly more anti-proliferation effect on BETi-resistant cells compared to parental controls (Figures S3E and S3F). Since the BETi-resistant cells displayed high AR activity, we investigated whether they were more sensitive to hormone deprivation. A remarkable decrease in the number of BETi-resistant cells compared to controls was observed in prolonged steroid-deficient conditions (Figure S3G). Moreover, unlike parental LNCaP cells, the AR and its target genes were not increased in the remaining cells after extended steroid deprivation, suggesting that BETi-resistant cells rely more on AR and its ligands for growth in addition to lack of feedback activation of AR signaling upon hormone deprivation (Figure S3H). Consequently, knockdown of AR had a more pronounced effect on the proliferation of BETi-resistant cells compared to the parental controls (Figures S3I and S3J). Next, we tested whether BETi-resistant cells were sensitive to enzalutamide. In a colony formation assay, enzalutamide exhibited enhanced anti-proliferation activity in the BETi-resistant cells (Figure 2L). These data suggest that a sequential BETi plus anti-androgen or CDK9 inhibitor combination therapy may benefit the enzalutamide refractory patient population.

Transcriptional Silencing of DDR Genes and Increased DNA Damage in BETi-Resistant Cells

In addition to its role as an epigenetic reader protein and transcriptional activator, BRD4 is known to act as an insulator of chromatin and prevent DNA damage (Floyd et al., 2013). DDR genes are responsible for the efficient repair of damaged DNA, and the pathway it constitutes protects the genome from low-level DNA damage induced by DNA replication, transcription, and other metabolic processes, as well as from exogenous damage (Tubbs and Nussenzweig, 2017). Deleterious germline or somatic aberrations in genes involved in DDR have been reported in PCa cells (Robinson et al., 2015), which has led to renewed interest in therapies targeting PARP, due to its synthetic lethal activity in DDR-deficient cells (Mateo et al., 2015; Pritchard et al., 2016). To determine whether DDR pathway genes are affected in the BETi-resistant cells, we

Figure 2. CDK9-Mediated Hyper-phosphorylation of AR and Increased AR Signaling in BETi-Resistant Cells

(A) GSEA plots of the AR signature in LNCaP BETi-resistant pools.

(B and C) qRT-PCR (B) and immunoblot (C) for KLK3 (PSA); transient treatment with JQ1 was for 48 hr.

(D) qRT-PCR for AR-regulated genes in the cells grown in steroid-depleted medium for 72 hr followed by stimulation with 10 nM DHT for indicated time points. *BRD4*, was used as a negative control. Data indicate mean ± SEM (n = 3) from one of the two independent experiments.

(E) Cells were treated as in (D), followed by immunoblotting with the pS81-AR antibody. Total AR and GAPDH were used as controls.

(F) Immunoblot showing pS81-AR, total AR, and GAPDH in cells treated with cycloheximide. S.E, short exposure; L.E, long exposure.

(G) Cells cultured in steroid-depleted medium for 72 hr were pretreated with vehicle or 5 μM CDK9 inhibitor for 1 hr, followed by 10 nM DHT for 24 hr and subsequent immunostaining with the pS81-AR specific antibody (red). Results are representative of three independent experiments. Scale bar, 40 μm.

(H) Quantification of the immunofluorescence signal (red).

(I) Immunoblot with indicated antibody with lysates from cells treated as in (G).

(J) qRT-PCR validation of CDK9 knockdown in LNCaP BETi-resistant cells grown in steroid-depleted media for 72 hr followed by vehicle or 10 nM DHT stimulation for 24 hr.

(K) Immunoblot analysis with protein extracts from (J) for the indicated targets.

(L) Colony formation assay in the presence of enzalutamide. Cells were cultured in the presence of vehicle, 1 μM enzalutamide, or 5 μM enzalutamide for 14 days followed by staining (left) and quantification (right).

Data indicate mean ± SEM. n = 6. *$p < 0.05$, by two-tailed Student's t test. NES, normalized enrichment score.

See also Figures S2 and S3.

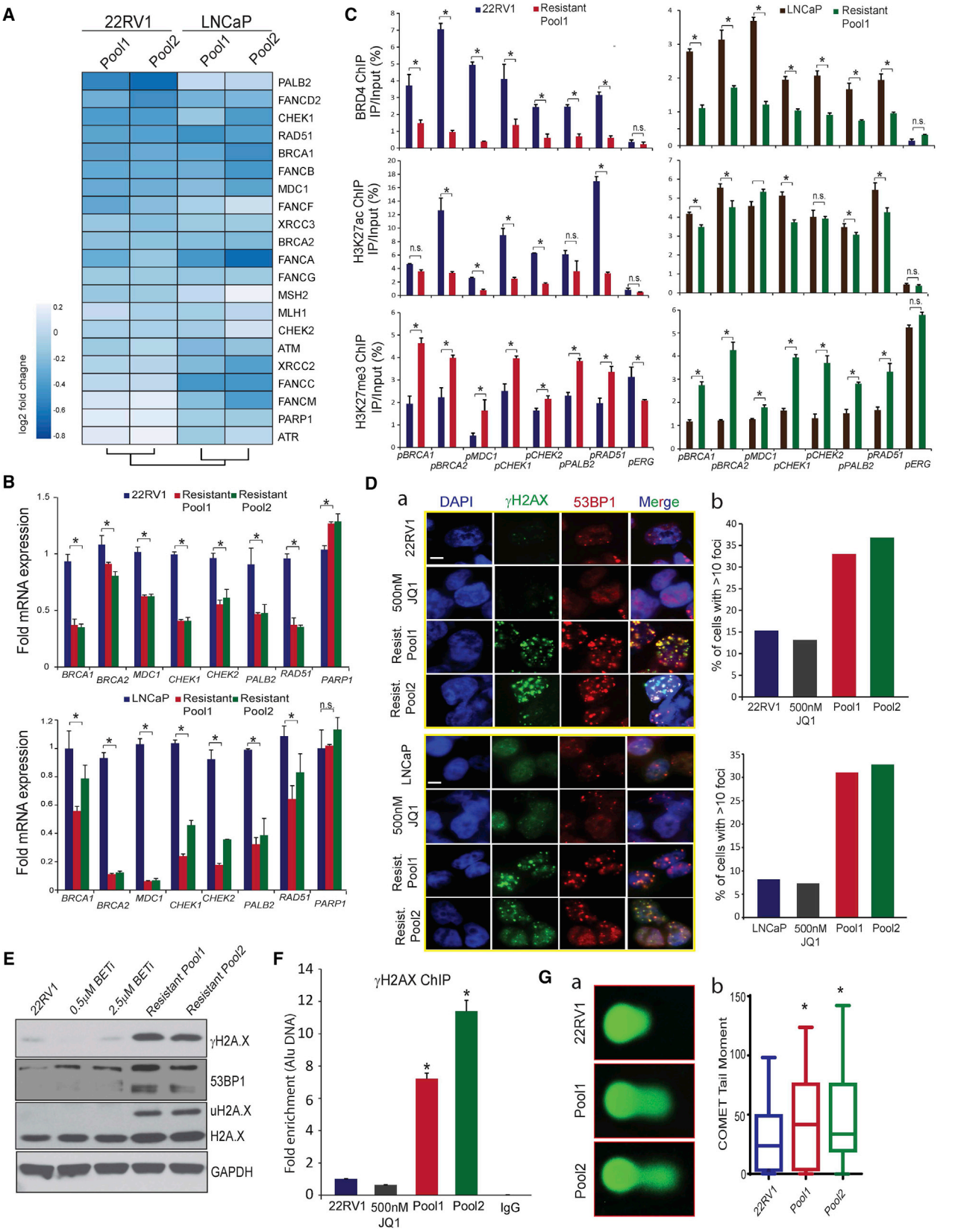

(legend on next page)

analyzed RNA-seq data from the resistant cells and found significant downregulation of a number of genes involved in homologous recombination (HR) and the non-homologous end joining (NHEJ) pathways of DDR (Figure 3A). Transcript levels for multiple DDR genes were decreased in BETi-resistant cells; however, the expression of *PARP1* was unchanged (Figures 3A and 3B). Expression and function of DDR genes are closely linked to cell-cycle checkpoints. However, we did not observe any significant accumulation of cell-cycle phase, except for a slight increase in G1 in the resistant cells, suggesting evasion of growth arrest in the BETi-resistant state (Figure S4). The transcriptional silencing of DDR genes in the resistant cells can be attributed, in part, to the observed decrease in BRD4 recruitment (due to chronic exposure to BETi) to its proximal promoters (Figures 3C and S5). This resulted in the loss of H3K27ac marks, and increased transcriptional silencing H3K27me3 marks, as determined by chromatin immunoprecipitation (ChIP) for BRD4, H3K27ac, and H3K27me3, followed by qPCR in both the BETi-resistant models (Figures 3C and S5). Furthermore, treating BETi-resistant 22Rv1 cells with GSK126, a small-molecule inhibitor against PRC2 catalytic subunit EZH2 that is responsible for H3K27me3, de-repressed the expression of DDR genes but had no effect on *PARP1* transcripts as expected with the lack of PARP1 downregulation in BETi-resistant cells (Figures S6A and S6B). These data suggest that the transcriptional silencing of these DDR genes is due to loss of BRD4 recruitment and accumulation of H3K27me3 marks mediated by the PRC2 complex in BETi-resistant cells. These observations may be specific to PCa cells, as resistance to BETi in the leukemia model was reported to be associated with decreased PRC2 activity due to transcriptional loss of SUZ12—a component of PRC2, leading to activation of the Wnt pathway (Rathert et al., 2015). Wnt pathway activation was not observed in our BETi-resistant transcriptome (data not shown). Next, we tested and found only partial restoration of DDR genes upon BETi withdrawal in the resistant cells, suggesting long-term transcriptional suppression (Figure S6C). Somatic loss-of-function mutations or reduced expression of DDR genes results in inefficient DNA repair and increased genomic instability in cancer cells (Curtin, 2012). γH2A.X and 53BP1 are the markers of DNA damage that accumulate and/or are modified in the vicinity of a DNA double-strand break to form microscopically visible sub-nuclear foci. To evaluate whether the BETi-resistant state leads to increased DNA damage, we conducted immunofluorescence staining to assess the presence of γH2A.X and 53BP1 foci and observed an increase in the number of γH2A.X and 53BP1 foci-positive cells in both the BETi-resistant models (Figure 3D). However, transient treatment with JQ1 22Rv1 did not result in any increase in γH2A.X and 53BP1 foci-positive cells (Figure 3D). The increase in γH2A.X and 53BP1 protein levels was apparent in the resistant pools, whereas cells with transient JQ1 treatment did not show any accumulation in these two DNA damage markers (Figure 3E). Interestingly, the ubiquitylated H2A.X, which surrounds the DNA double-strand breaks, was evident only in the BETi-resistant cells. Furthermore, by ChIP-qPCR, increased enrichment of γH2A.X was observed on Alu repeats, suggesting widespread DNA breaks in the BETi resistance cells, whereas transient JQ1 treatment did not show enrichment (Figure 3F). These data suggest that the decrease in the levels of DDR genes and associated DNA damage is specific to cells that have acquired resistance to BETi. After demonstrating the accumulation of markers of DNA damage, we sought to confirm the presence of DNA double-strand breaks by directly analyzing cellular DNA for fragmentation using the COMET assay. As with the γH2A.X and 53BP1 foci formation, significantly increased longer tails were observed in the BETi-resistant cell than those found in parental controls (Figure 3G). No such increase in COMET tail moment was observed in cells transiently treated with JQ1 (Figure S6D). These observations suggest that the DDR-deficient state with associated genomic instability is specific to acquired BETi-resistant cells that might be amenable to DDR pathway drugs such as PARP inhibitors.

Increased Sensitivity to PARP Inhibitors and Cisplatin in BETi-Resistant Cells

PARP is a major player in the DDR, and its enzymatic activity is critical in mediating the repair of single-strand breaks (SSBs) through the DNA base excision repair (BER) pathway. When PARP activity is inhibited, unrepaired SSBs degenerate to double-strand breaks, which can no longer be repaired in the HR-deficient cells, leading to death (Curtin, 2012). Additionally, the mechanism of death in HR-deficient cells is thought to be due to PARP trapping on chromatin by PARP inhibitors (Murai et al., 2012). Transcriptional downregulation of DDR genes and sensitivity to PARP inhibition have been reported in triple-negative breast cancer (Ibrahim et al., 2012). Since we observed an increase in double-strand breaks and decreased expression of HR genes, a quasi-"BRCAness" state, in the BETi-resistant cells, we investigated their sensitivity to PARP inhibitors. Cells were treated with olaparib, an FDA-approved PARP inhibitor, and showed a dose-dependent reduction in PARylated proteins

Figure 3. Transcriptional Silencing of DDR Genes Due to Reduced BRD4 Recruitment and High H3K27me3 Leads to Increased DNA Damage

(A) RNA-seq (FPKM) heatmap of downregulated genes associated with DDR.

(B) qRT-PCR for the indicated DDR genes.

(C) ChIP-qPCR analysis of BRD4, H3K27ac, and H3K27me3 at the indicated gene promoter. Primer set amplifying a region around the transcription start site (TSS) of *ERG* gene (*pERG*) was used as a control.

(D) a: representative images of immunofluorescent staining of indicated cells with γH2A.X (green) and 53BP1 (red). The nucleus was visualized by DAPI (blue). b: percentage of cells that show more than 10 foci/nuclei. Transient treatment of parental cells with 500 nM JQ1 was for 48 hr. Scale bar, 10 μm.

(E) Immunoblot analysis for γ-H2A.X and 53BP1; transient treatment with JQ1 was for 48 hr. Data are representative of two independent experiments.

(F) ChIP-qPCR analysis of γH2A.X bound to Alu repeats.

(G) a and b: double-strand breaks in BETi-resistant cells. COMET assays were done in the parental and BETi-resistant 22Rv1 cells (n = 3; error bars indicate SEM). *$p < 0.05$, by two-tailed Student's t test.

See also Figures S4, S5, and S6.

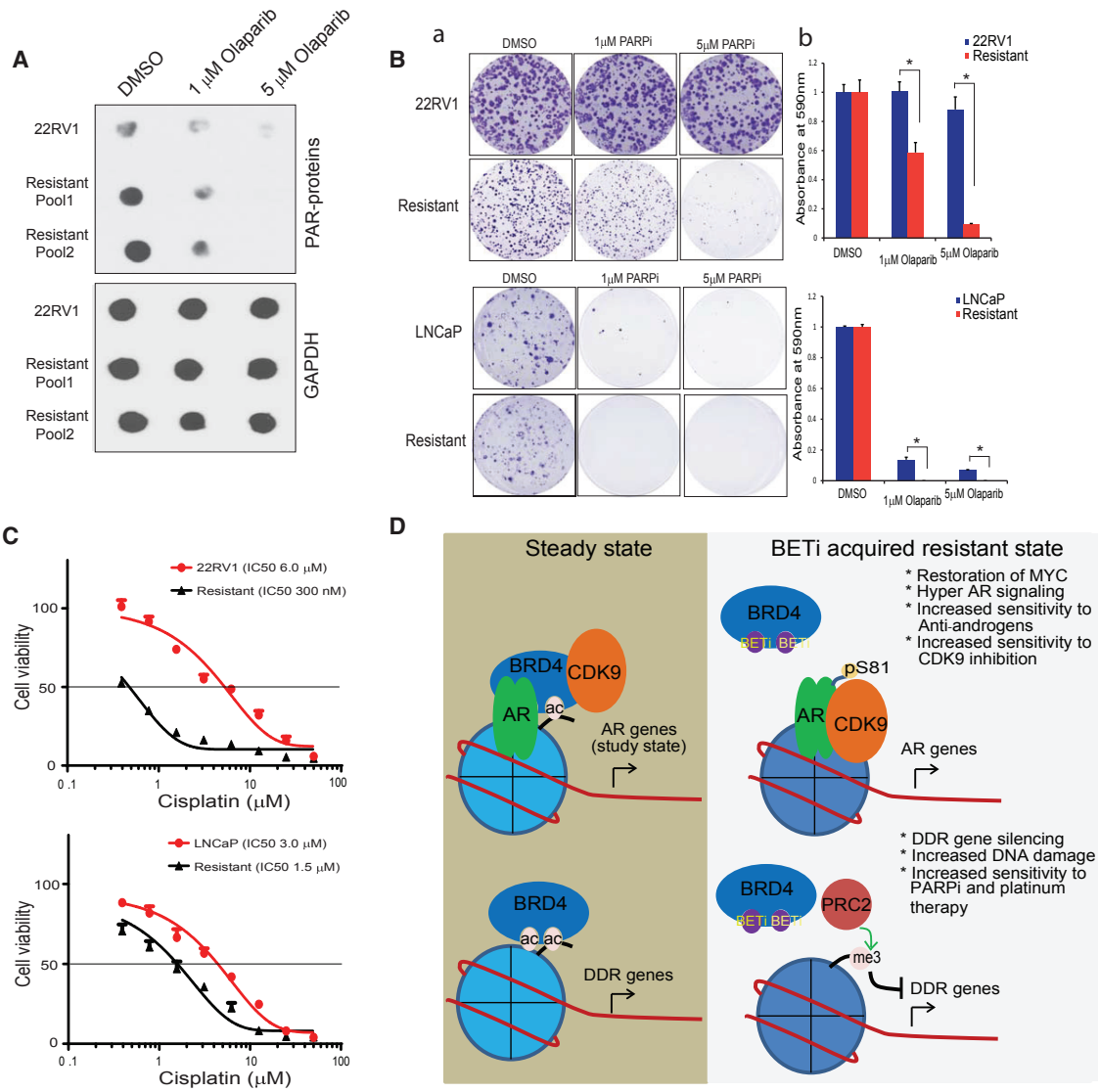

Figure 4. PARP Hyperactivity and Increased Sensitivity to PARP Inhibitor in BETi-Resistant Cells

(A) Control and BETi-resistant 22RV1 cells were treated with 1 μM and 5 μM olaparib for 48 hr. Total lysates were used for dot-blot analysis with anti-PAR antibody. GAPDH was used as a control.

(B) Colony formation assays in the presence of olaparib. Cells were cultured in the presence or absence of 1 μM and 5 μM of olaparib for 14 days followed by staining (a) and quantification (b). Data indicate mean ± SEM (n = 6). *$p < 0.05$, by two-tailed Student's t test.

(C) Representative dose-response curves for cells treated with cisplatin.

(D) Schematic depicting the mechanisms of acquired resistance to BET-inhibitor therapy in CRPC.

in the control cells (Figure 4A). High PARP activity is associated with DNA damage, and this was evident in the BETi-resistant cells that showed an increase in PAR-protein levels that were potently inhibited by olaparib. In a colony formation assay, BETi-resistant 22Rv1 cells were sensitive to olaparib, whereas its parental controls were unaffected (Figure 4B). Although LNCaP cells displayed sensitivity to olaparib, the BETi-resistant derivative cells exhibited greater sensitivity to treatment (Figure 4B). Platinum sensitivity is a strong predictor of "BRCAness" in cancers, including PCa (Cheng et al., 2016). Therefore, we tested and found a remarkable increase in cisplatin sensitivity in BETi-resistant cells (Figure 4C). These data are in line with the clinical observation that HR-deficient patients respond to platinum-based therapies.

Together, this work provides insights on the mechanism of acquired resistance to BETi and parallel activation of growth-sustaining pathways in two different models of CRPC. Our study has uncovered the dispensable nature of BRD4 proteins in BETi-resistant cells, leading to the restoration of MYC and adaptive reactivation of CDK9-mediated AR signaling, as well as PRC2-induced transcriptional silencing of DDR genes, resulting in "BRCAness" (Figure 4D). These findings are analogous to those

of other reports where transcriptional plasticity was proposed to be the major mechanism of acquired resistance to BETi (Fong et al., 2015; Rathert et al., 2015; Shu et al., 2016). Further research efforts will be directed toward understanding the upstream events causing the CDK9-mediated AR hyper-phosphorylation/stability and the functional involvement of MYC in sustaining the AR signaling in BETi-resistant cells. Moreover, additional efforts will be directed toward understanding the underlying mechanism causing the continued repression/reactivation of genes, even after BETi withdrawal, as well as selective transcriptional silencing of DDR genes by the PRC2 complex in response to sustained BET inhibition. In conclusion, our study provides a strong rationale for therapies that include BETi in combination with CDK9 inhibitors, anti-androgen enzalutamide, PARP inhibitors, and platinum-based drugs, upfront or in BETi-refractory disease for CRPC patients in the clinic.

EXPERIMENTAL PROCEDURES

Cell Culture and Development of BETi-Resistant Lines

22RV1 and LNcaP prostate cancer cells were cultured in RPMI 1640 (GIBCO) supplemented with 10% (v/v) fetal bovine serum (FBS) (GIBCO). BETi (JQ1)-resistant lines were developed by culturing in the aforementioned media with half-maximum inhibitory concentrations (IC_{50}) of the drug (100 nM and 200 nM for LNcaP and 22RV1, respectively) for over a period of 14–16 weeks. Surviving BETi-resistant polyclonal pools were maintained in JQ1 throughout. All experiments for BETi-resistant pools were done in presence of JQ1, except those in which other BET inhibitors (ZBC260, HJB97, I-BET762, and OTX-015) were used. The primer sequences for SYBR Green PCR, the Alu primer probe for TaqMan PCR, and antibodies used is provided in Table S2.

Statistical Analysis

All statistical analysis was carried out using GraphPad Prism. For quantitative data, treatment groups were reported as mean ± SEM and compared using the unpaired Student's t test.

DATA AND SOFTWARE AVAILABILITY

The accession number for the RNA-seq data reported in this paper is GEO: GSE103082.

SUPPLEMENTAL INFORMATION

Supplemental Information includes Supplemental Experimental Procedures, six figures, and two tables and can be found with this article online at https://doi.org/10.1016/j.celrep.2018.02.011.

ACKNOWLEDGMENTS

We thank Drs. S. Ryeom and Z. Jabeen for critically reading the manuscript. This work was supported by a Department of Defense Idea Development award to (W81XWH-17-1-0404) I.A.A.

AUTHOR CONTRIBUTIONS

I.A.A. conceived the work and designed the experiments. A.P., P.N.G., and I.A.A. performed the experiments and acquired the data. S.W. provided compounds. I.A.A. interpreted the data, prepared the figures, and wrote the manuscript. All authors discussed the results and commented on the manuscript.

DECLARATION OF INTERESTS

The authors declare no competing interests.

Received: August 6, 2017
Revised: December 20, 2017
Accepted: February 1, 2018
Published: February 27, 2018

REFERENCES

Antonarakis, E.S., Lu, C., Wang, H., Luber, B., Nakazawa, M., Roeser, J.C., Chen, Y., Mohammad, T.A., Chen, Y., Fedor, H.L., et al. (2014). AR-V7 and resistance to enzalutamide and abiraterone in prostate cancer. N. Engl. J. Med. *371*, 1028–1038.

Asangani, I.A., Dommeti, V.L., Wang, X., Malik, R., Cieslik, M., Yang, R., Escara-Wilke, J., Wilder-Romans, K., Dhanireddy, S., Engelke, C., et al. (2014). Therapeutic targeting of BET bromodomain proteins in castration-resistant prostate cancer. Nature *510*, 278–282.

Asangani, I.A., Wilder-Romans, K., Dommeti, V.L., Krishnamurthy, P.M., Apel, I.J., Escara-Wilke, J., Plymate, S.R., Navone, N.M., Wang, S., Feng, F.Y., and Chinnaiyan, A.M. (2016). BET bromodomain inhibitors enhance efficacy and disrupt resistance to AR antagonists in the treatment of prostate cancer. Mol. Cancer Res. *14*, 324–331.

Belkina, A.C., and Denis, G.V. (2012). BET domain co-regulators in obesity, inflammation and cancer. Nat. Rev. Cancer *12*, 465–477.

Chan, S.C., Selth, L.A., Li, Y., Nyquist, M.D., Miao, L., Bradner, J.E., Raj, G.V., Tilley, W.D., and Dehm, S.M. (2015). Targeting chromatin binding regulation of constitutively active AR variants to overcome prostate cancer resistance to endocrine-based therapies. Nucleic Acids Res. *43*, 5880–5897.

Chen, C.D., Welsbie, D.S., Tran, C., Baek, S.H., Chen, R., Vessella, R., Rosenfeld, M.G., and Sawyers, C.L. (2004). Molecular determinants of resistance to antiandrogen therapy. Nat. Med. *10*, 33–39.

Chen, S., Gulla, S., Cai, C., and Balk, S.P. (2012). Androgen receptor serine 81 phosphorylation mediates chromatin binding and transcriptional activation. J. Biol. Chem. *287*, 8571–8583.

Cheng, H.H., Pritchard, C.C., Boyd, T., Nelson, P.S., and Montgomery, B. (2016). Biallelic inactivation of BRCA2 in platinum-sensitive metastatic castration-resistant prostate cancer. Eur. Urol. *69*, 992–995.

Curtin, N.J. (2012). DNA repair dysregulation from cancer driver to therapeutic target. Nat. Rev. Cancer *12*, 801–817.

Delmore, J.E., Issa, G.C., Lemieux, M.E., Rahl, P.B., Shi, J., Jacobs, H.M., Kastritis, E., Gilpatrick, T., Paranal, R.M., Qi, J., et al. (2011). BET bromodomain inhibition as a therapeutic strategy to target c-Myc. Cell *146*, 904–917.

Floyd, S.R., Pacold, M.E., Huang, Q., Clarke, S.M., Lam, F.C., Cannell, I.G., Bryson, B.D., Rameseder, J., Lee, M.J., Blake, E.J., et al. (2013). The bromodomain protein Brd4 insulates chromatin from DNA damage signalling. Nature *498*, 246–250.

Fong, C.Y., Gilan, O., Lam, E.Y., Rubin, A.F., Ftouni, S., Tyler, D., Stanley, K., Sinha, D., Yeh, P., Morison, J., et al. (2015). BET inhibitor resistance emerges from leukaemia stem cells. Nature *525*, 538–542.

Gordon, V., Bhadel, S., Wunderlich, W., Zhang, J., Ficarro, S.B., Mollah, S.A., Shabanowitz, J., Hunt, D.F., Xenarios, I., Hahn, W.C., et al. (2010). CDK9 regulates AR promoter selectivity and cell growth through serine 81 phosphorylation. Mol. Endocrinol. *24*, 2267–2280.

Ibrahim, Y.H., García-García, C., Serra, V., He, L., Torres-Lockhart, K., Prat, A., Anton, P., Cozar, P., Guzmán, M., Grueso, J., et al. (2012). PI3K inhibition impairs BRCA1/2 expression and sensitizes BRCA-proficient triple-negative breast cancer to PARP inhibition. Cancer Discov. *2*, 1036–1047.

Kurimchak, A.M., Shelton, C., Duncan, K.E., Johnson, K.J., Brown, J., O'Brien, S., Gabbasov, R., Fink, L.S., Li, Y., Lounsbury, N., et al. (2016). Resistance to BET bromodomain inhibitors is mediated by kinome reprogramming in ovarian cancer. Cell Rep. *16*, 1273–1286.

Lockwood, W.W., Zejnullahu, K., Bradner, J.E., and Varmus, H. (2012). Sensitivity of human lung adenocarcinoma cell lines to targeted inhibition of BET epigenetic signaling proteins. Proc. Natl. Acad. Sci. USA *109*, 19408–19413.

Lu, H., Xue, Y., Yu, G.K., Arias, C., Lin, J., Fong, S., Faure, M., Weisburd, B., Ji, X., Mercier, A., et al. (2015). Compensatory induction of MYC expression by sustained CDK9 inhibition via a BRD4-dependent mechanism. eLife *4*, e06535.

Mateo, J., Carreira, S., Sandhu, S., Miranda, S., Mossop, H., Perez-Lopez, R., Nava Rodrigues, D., Robinson, D., Omlin, A., Tunariu, N., et al. (2015). DNA-repair defects and olaparib in metastatic prostate cancer. N. Engl. J. Med. *373*, 1697–1708.

Murai, J., Huang, S.Y., Das, B.B., Renaud, A., Zhang, Y., Doroshow, J.H., Ji, J., Takeda, S., and Pommier, Y. (2012). Trapping of PARP1 and PARP2 by clinical PARP inhibitors. Cancer Res. *72*, 5588–5599.

Pritchard, C.C., Mateo, J., Walsh, M.F., De Sarkar, N., Abida, W., Beltran, H., Garofalo, A., Gulati, R., Carreira, S., Eeles, R., et al. (2016). Inherited DNA-repair gene mutations in men with metastatic prostate cancer. N. Engl. J. Med. *375*, 443–453.

Raina, K., Lu, J., Qian, Y., Altieri, M., Gordon, D., Rossi, A.M., Wang, J., Chen, X., Dong, H., Siu, K., et al. (2016). PROTAC-induced BET protein degradation as a therapy for castration-resistant prostate cancer. Proc. Natl. Acad. Sci. USA *113*, 7124–7129.

Rathert, P., Roth, M., Neumann, T., Muerdter, F., Roe, J.S., Muhar, M., Deswal, S., Cerny-Reiterer, S., Peter, B., Jude, J., et al. (2015). Transcriptional plasticity promotes primary and acquired resistance to BET inhibition. Nature *525*, 543–547.

Robinson, D., Van Allen, E.M., Wu, Y.M., Schultz, N., Lonigro, R.J., Mosquera, J.M., Montgomery, B., Taplin, M.E., Pritchard, C.C., Attard, G., et al. (2015). Integrative clinical genomics of advanced prostate cancer. Cell *161*, 1215–1228.

Shu, S., Lin, C.Y., He, H.H., Witwicki, R.M., Tabassum, D.P., Roberts, J.M., Janiszewska, M., Huh, S.J., Liang, Y., Ryan, J., et al. (2016). Response and resistance to BET bromodomain inhibitors in triple-negative breast cancer. Nature *529*, 413–417.

Tubbs, A., and Nussenzweig, A. (2017). Endogenous DNA damage as a source of genomic instability in cancer. Cell *168*, 644–656.

Watson, P.A., Arora, V.K., and Sawyers, C.L. (2015). Emerging mechanisms of resistance to androgen receptor inhibitors in prostate cancer. Nat. Rev. Cancer *15*, 701–711.

Wyce, A., Degenhardt, Y., Bai, Y., Le, B., Korenchuk, S., Crouthame, M.C., McHugh, C.F., Vessella, R., Creasy, C.L., Tummino, P.J., and Barbash, O. (2013). Inhibition of BET bromodomain proteins as a therapeutic approach in prostate cancer. Oncotarget *4*, 2419–2429.

Zhou, B., Hu, J., Xu, F., Chen, Z., Bai, L., Fernandez-Salas, E., Lin, M., Liu, L., Yang, C.Y., Zhao, Y., et al. (2017). Discovery of a small-molecule degrader of bromodomain and extra-terminal (BET) proteins with picomolar cellular potencies and capable of achieving tumor regression. J. Med. Chem.

Cell Reports, Volume *22*

Supplemental Information

Resistance to BET Inhibitor Leads to Alternative Therapeutic Vulnerabilities in Castration-Resistant Prostate Cancer

Aishwarya Pawar, Paradesi Naidu Gollavilli, Shaomeng Wang, and Irfan A. Asangani

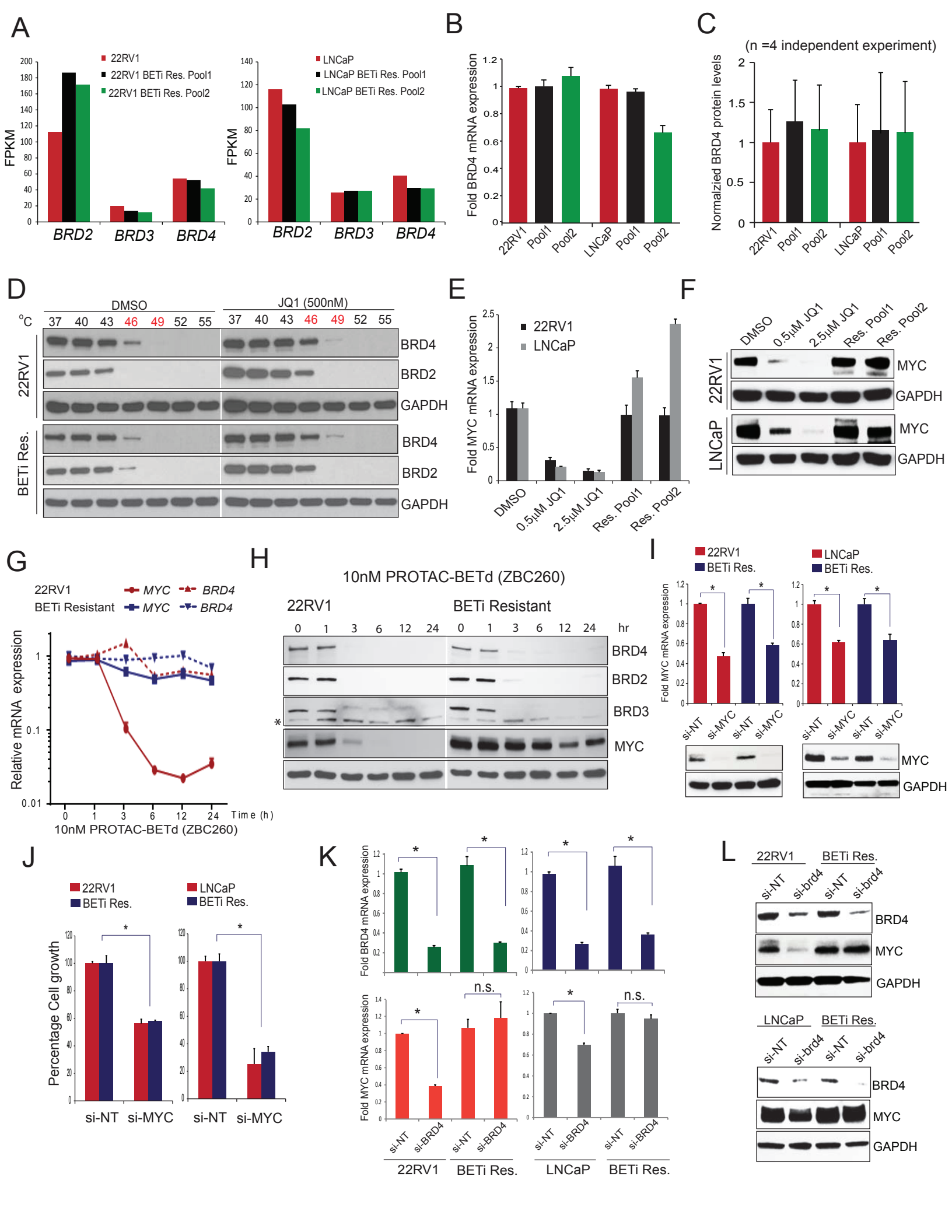
A
22RV1
22RV1 BETi Res. Pool1
22RV1 BETi Res. Pool2
FPKM
BRD2
BRD3
BRD4
LNCaP
LNCaP BETi Res. Pool1
LNCaP BETi Res. Pool2
B
Fold BRD4 mRNA expression
22RV1
Pool1
Pool2
LNCaP
C
(n =4 independent experiment)
Normalzied BRD4 protein levels
D
DMSO
JQ1 (500nM)
°C
37 40 43 46 49 52 55
22RV1
BETi Res.
BRD4
BRD2
GAPDH
E
Fold MYC mRNA expression
22RV1
LNCaP
DMSO
0.5μM JQ1
2.5μM JQ1
Res. Pool1
Res. Pool2
F
DMSO
0.5μM JQ1
2.5μM JQ1
Res. Pool1
Res. Pool2
22RV1
LNCaP
MYC
GAPDH
G
22RV1
BETi Resistant
MYC
BRD4
Relative mRNA expression
Time (h)
10nM PROTAC-BETd (ZBC260)
H
10nM PROTAC-BETd (ZBC260)
22RV1
BETi Resistant
0 1 3 6 12 24 0 1 3 6 12 24 hr
BRD4
BRD2
BRD3
MYC
I
22RV1
BETi Res.
LNCaP
BETi Res.
Fold MYC mRNA expression
si-NT
si-MYC
MYC
GAPDH
J
22RV1
BETi Res.
LNCaP
BETi Res.
Percentage Cell growth
si-NT
si-MYC
K
Fold BRD4 mRNA expression
Fold MYC mRNA expression
n.s.
si-NT
si-BRD4
22RV1
BETi Res.
LNCaP
BETi Res.
L
22RV1
BETi Res.
si-NT
si-brd4
BRD4
MYC
GAPDH
LNCaP
BETi Res.

Figure S1. BRD4 in BETi-resistant CRPC cells. Realted to Figure 1. (A) No significant change in the expression of BRD2, BRD3 and BRD4 transcripts in BETi-resistant cells. Bar graph showing fpkm (fragments per kilobase million) values from RNA-seq counts for BRD2, BRD3 and BRD4 transcripts in the parental 22Rv1 and LNCaP cells and their respective BETi-resistant derivatives. qRT-PCR for BRD4 transcript levels in BETi-resistant lines compared to 22Rv1 and LNCaP parental lines. Data show mean ± s.d. (n = 3). (C) No significant change in the BRD4 protein levels in the BETi-resistant cells. Image J quantification of 4 independent immunoblots for BRD4 protein levels in the BETi-resistant lines compared to parental cells. GAPDH levels were used to normalize the data. Mean ± s.d. is shown. (D) No change in JQ1 binding to BRD4 and BRD2 proteins in BETi-resistant 22Rv1 cells. Parental 22Rv1 and its BETi-resistant derivative cells were treated with 500nM JQ1 for 3hr and incubated at indicated temperatures for CETSA (cellular thermal shift assay). Cells were lysed and soluble proteins were detected by immunoblotting with the indicated antibody. Shown are representative blots (n=2). Temperature in red indicates the stability of the targets in the JQ1 treated cells. (E) and (F) Restoration of MYC expression in BETi-resistant cells. qRT-PCR and immunoblot MYC expression in BETi-resistant cells, compared to parental control treated with DMSO or JQ1 for 48h. Loss of MYC expression was evident on transient treatment with JQ1. (G) and (H) Lack of MYC downregulation on treatment with PROTAC-BET degrader in the BETi-resistant cells despite complete degradation of all three BET proteins. qRT-PCR analysis for MYC and BRD4 mRNA in the 22Rv1 and BETi-resistant cells treated with 10nM compound ZBC260 for the indicated time point. Immunoblot showing BRD2, BRD3, BRD4, MYC and GAPDH levels. * – non-specific band. (I) and (J) MYC knockdown reduces the growth of BETi-resistant and parental cells. qRT-PCR and immunoblot validation of siRNA MYC knockdown in 22Rv1 and LNCaP cells and their respective BETi-resistant lines. Equal number of cells were seeded in 24-well plates 48h post-transfection with si-NT or si-MYC and counted after 6 days. (K) Knockdown of BRD4 does not affect MYC expression in BETi-resistant cells. qRT-PCR analysis for BRD4 and MYC mRNA in cells transfected with siBRD4 or non-target (NT) siRNA. Data show mean ± s.e.m. (n = 3). (L) Immunoblot for BRD4 and MYC in the siBRD4 or si-NT transfected cells as in K. Note the lack of change in the MYC protein expression upon BRD4 knockdown in the BETi-resistant cells. * $P < 0.05$ by two-tailed Student's t-test. n.s., not significant.

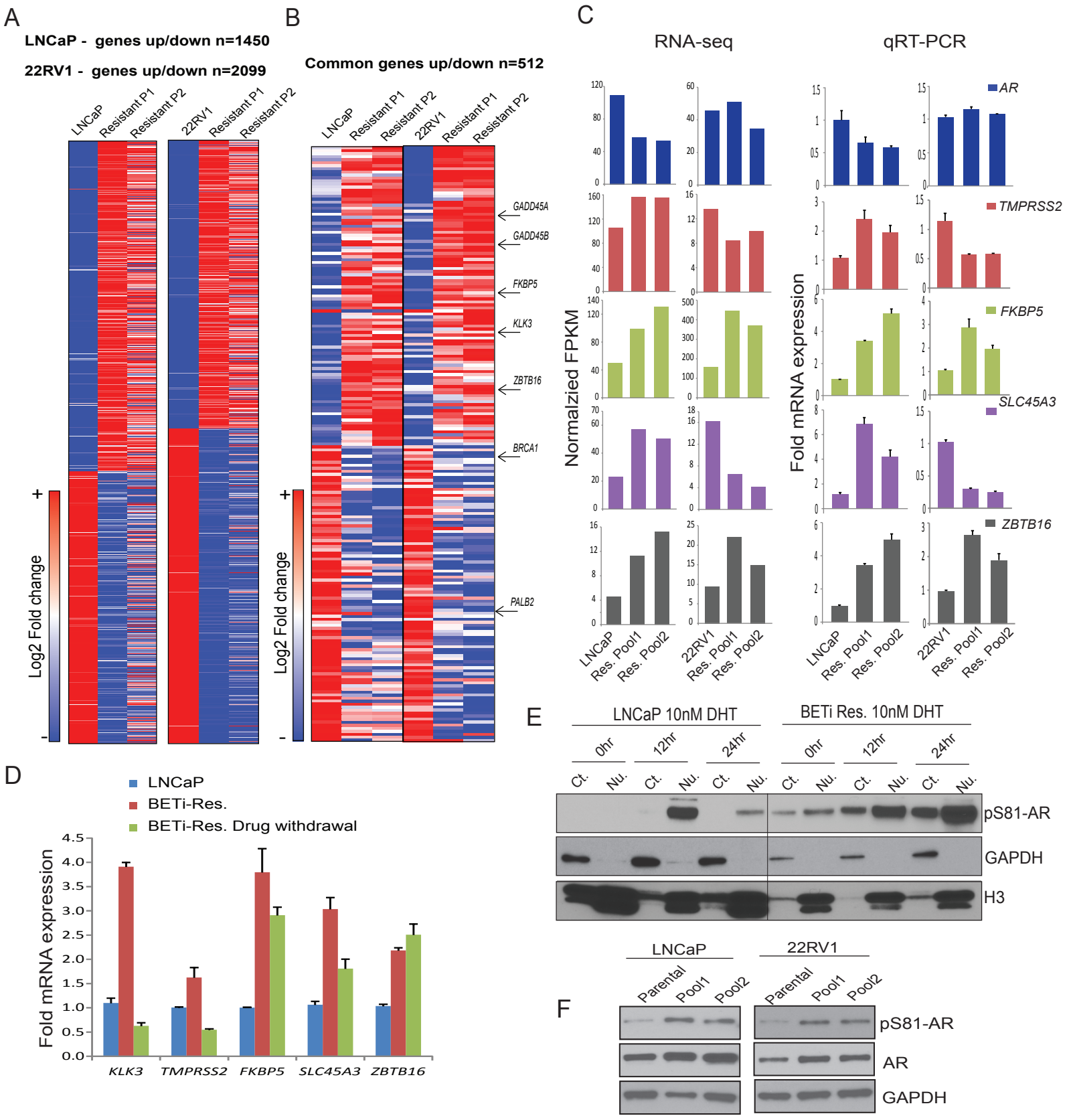

Figure S2. Increased AR signaling in BETi-resistant cells. Related to Figure 2. (A) and (B), Heat map showing the fold change in expression levels of transcripts identified as two fold upregulated and two fold downregulated in two independent resistant pools. Fold changes were calculated from normalized RNA-seq counts. (C) RNAseq FPKM values and qRT-PCR validation of AR and indicated AR target genes in the BETi-resistant pools and parental cells. (D) Partial reversal of AR-target genes after drug withdrawal. qRT-PCR for the indicated AR-target genes in parental LNCaP and BETi-resistant cells before after drug withdrawal for 48h. (E) Increased nuclear pS81-AR in BETi-resistant cells. Immunoblot analysis with cytoplasmic and nuclear fraction for pS81-AR in the DHT treated LNCaP and BETi-resistant cells following 3 days of steroid deprivation. (F) Immunoblot showing pS81-AR, total AR, and GAPDH in the indicated cells.

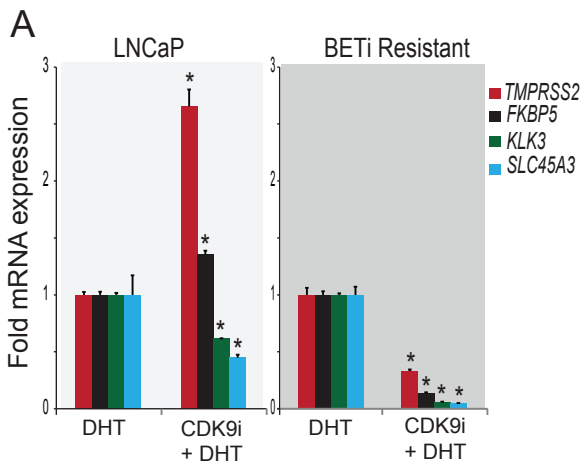

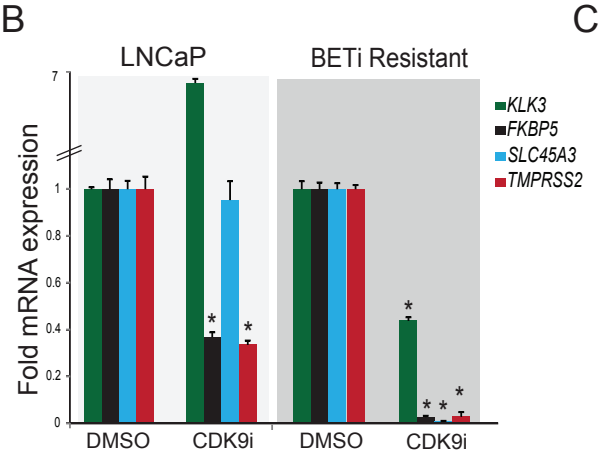

C

LDC000067 (CDK9i) IC50 (μM)

Cells	22RV1	LNCaP
Parental	8	2.5
BETi Res.	2.5	1

Dinaciclib IC50 (nM)
(CDK1,2,5 and 9 specific inhibitor)

Cells	22RV1	LNCaP
Parental	12	12
BETi Res.	8	4

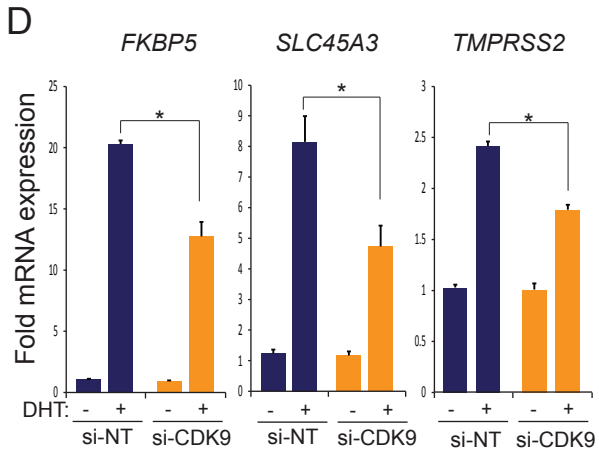

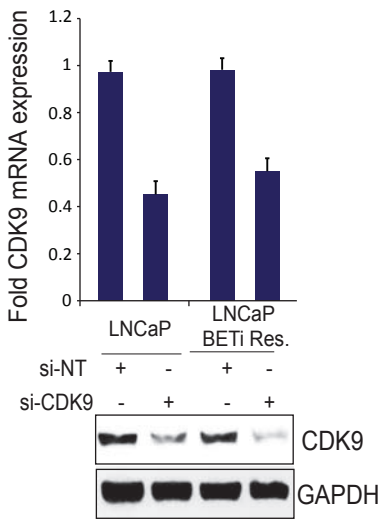

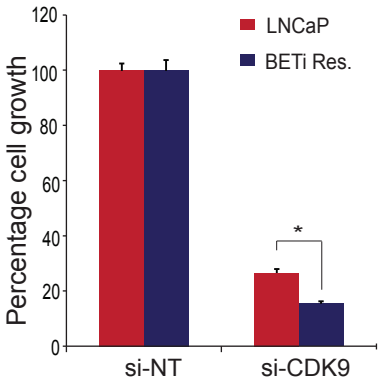

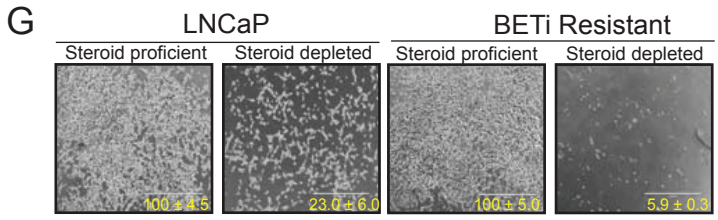

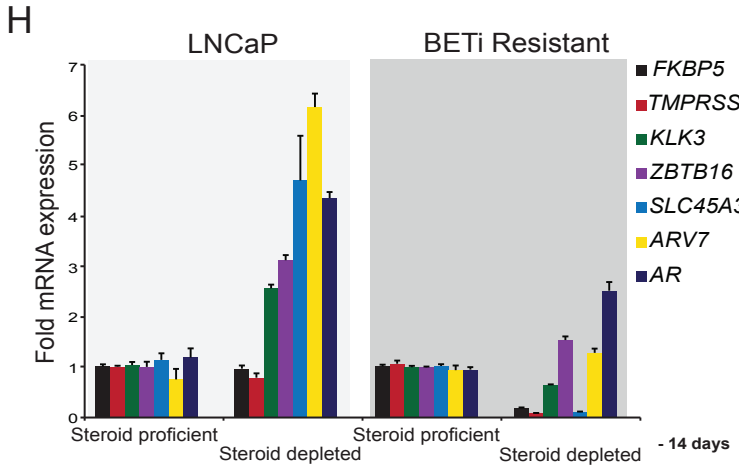

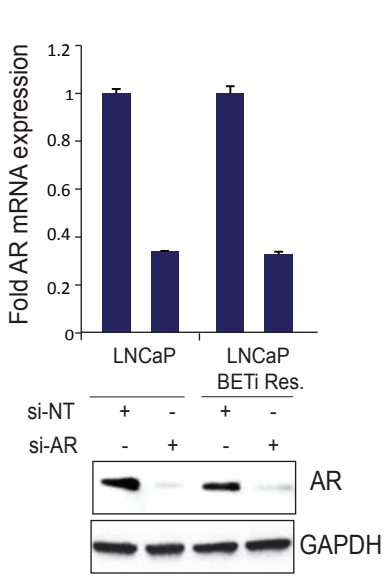

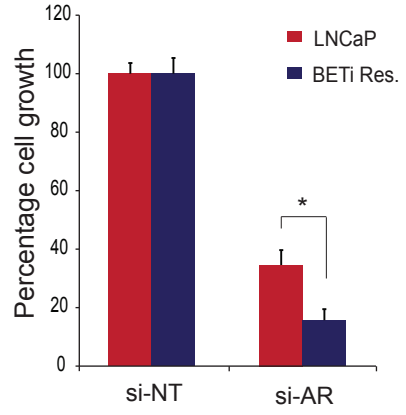

Figure S3. Increased sensitivity to CDK9 or AR blockade in BETi-resistant cells. Related to Figure 2. (A) More pronounced downregulation of DHT induced AR-target genes by CDK9i in BETi-resistant cells. qRT-PCR analysis of AR-regulated genes in LNCaP and LNCaP BETi-resistant cells treated with DHT alone or 10μM CDK9 inhibitor plus DHT for 24h after 3days of steroid deprivation. Representative data shown with mean ± S.E. (n =3) from one of the two independent experiments. (B) qRT-PCR for the indicated AR-targets in cells growing in normal media treated with DMSO or 10μM CDK9i (LDC000067) for 24h. (C) Table showing growth IC50 concentration for CDK9 specific inhibitor LDC000067 and Dinaciclib (CDK1, 2, 5, 9 inhibitor) in parental and BETi-resistant cells. Cells were incubated with compounds for 4 days followed by cell viability assay. (D) qRT-PCR analysis of AR-target genes in LNCaP BETi-resistant cells after siRNA knockdown of CDK9, grown in steroid depleted media followed by vehicle or 10nM DHT stimulation as in Figure 2J and 2K. (E) and (F) Increased sensitivity to CDK9 knockdown in BETi-resistant cells. qRT-PCR and immunoblot validation of CDK9 knockdown in LNCaP and BETi-resistant cells. Equal number of cells were seeded in 24-well plates 48h post-transfection with si-NT or si-CDK9 and counted after 6 days. (G) Increased sensitivity to steroid deprivation in BETi-resistant cells. Bright-field images of LNCaP and LNCaP BETi-resistant cells grown in steroid-proficient or steroid-depleted media for 14-days. Inset shows cell viability count using CellTiter-Glo from triplicate wells of a six well. (H) AR and its target gene expression in the cell as in G. Note the overexpression of AR, AR-v7 and many of its target genes in the steroid-depleted LNCaP cells whereas no such increase was observed in the LNCaP BETi-resistant cells. * $P < 0.05$ by two-tailed Student's t-test. (I) qRT-PCR and immunoblot validation of siRNA knockdown of AR in the indicated cells. (J) Quatification of cell growth assay showing more pronounced reduction of growth in BETi resistant LNCaP cells on knockdown of AR compared to parental controls.

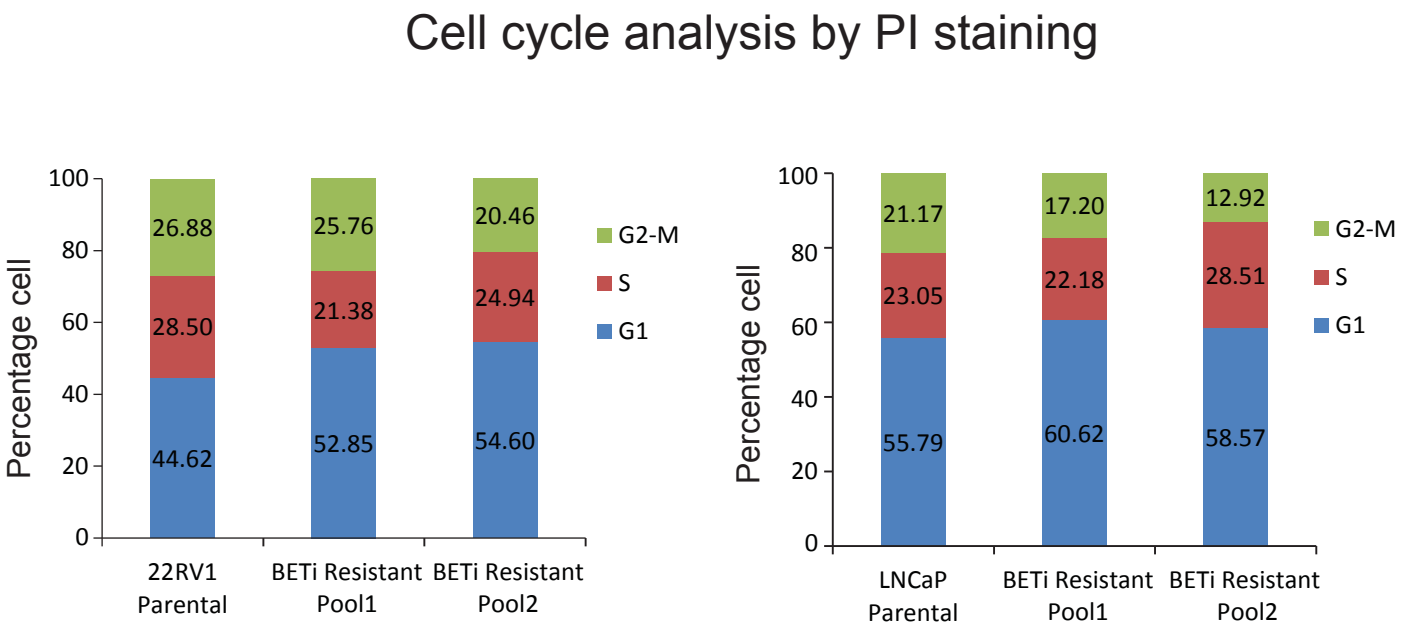

Figure S4: Cell cycle analysis of parental and BETi-resistant 22Rv1 and LNCaP cells. Related to Figure 3.

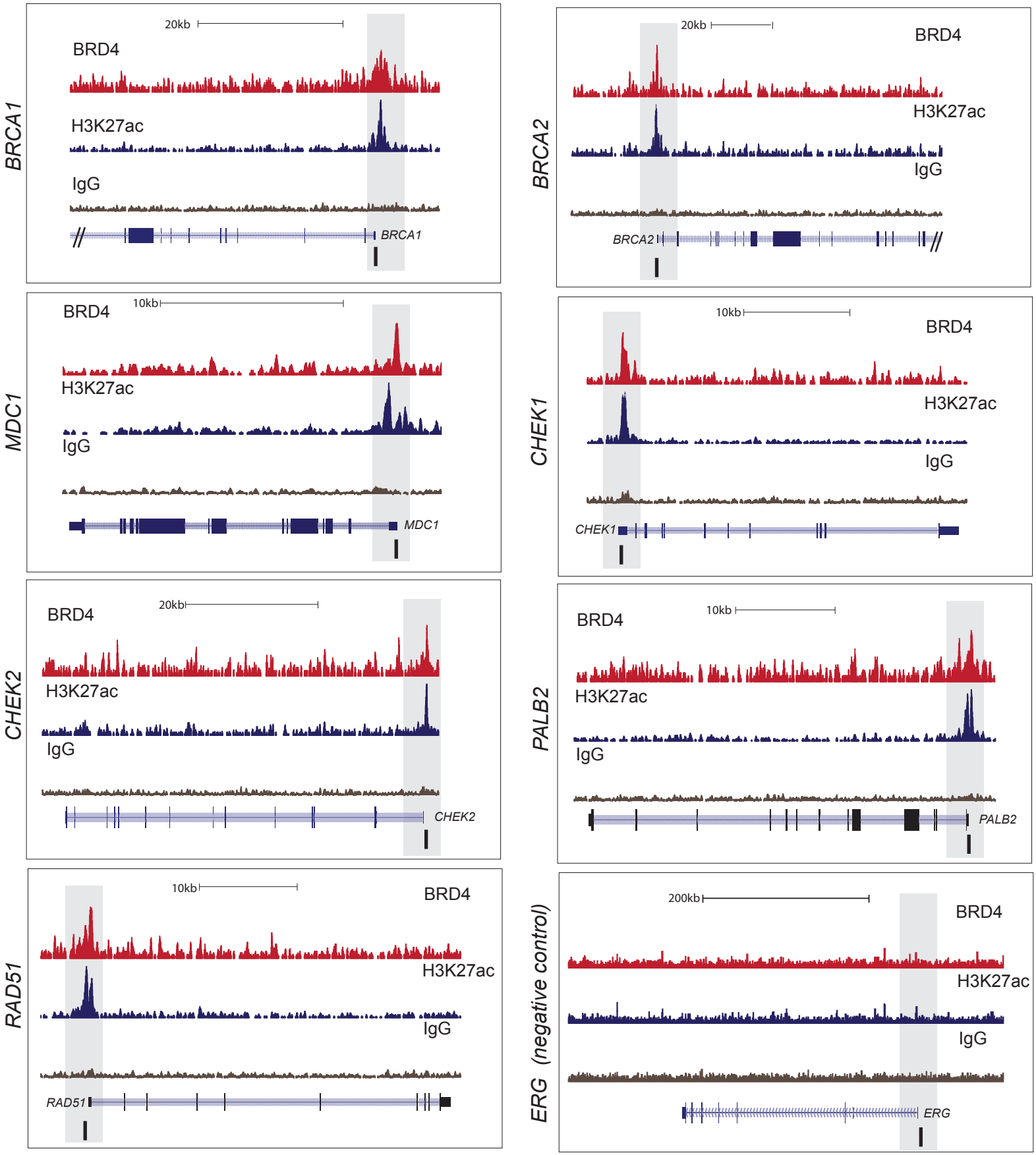

Figure S5: BRD4 occupies the DDR gene promoters. Related to Figure 3. BRD4 binding on the proximal promoter/TSS of multiple DDR genes. UCSC genome browser view of BRD4 and H3K27ac ChIP-seq tracks in LNCaP cells. Shaded area shows the BRD4 and H3K27ac peak and the black bar below is the region used to amplify for ChIP-qPCR validation shown in Figure 3C. ERG which is not expressed in LNCaP cells serves as a negative control.

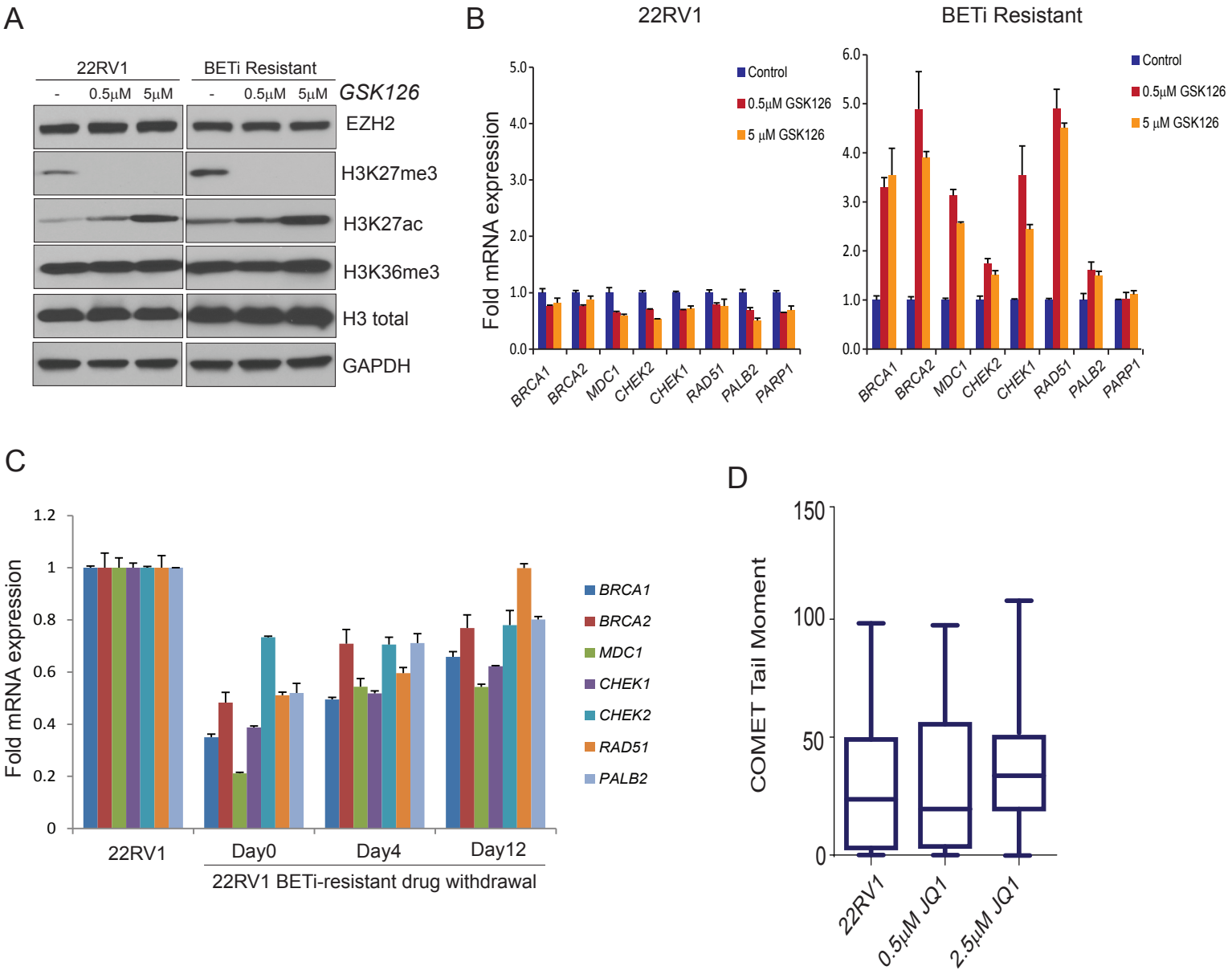

Figure S6: EZH2 inhibition de-represses multiple DDR genes in BETi-resistant cells. Related to Figure 3. (A) EZH2 inhibition reduces H3K27me3 and concomitant increase in H3K27ac marks. Immunoblot analysis of EZH2 and different histone methylation marks in the parental and BETi-resistant 22Rv1 cells treated with DMSO or two different concentration of EZH2i (GSK126) for 4 days. Total histone H3 and GAPDH served as loading controls. (B) qRT-PCR for indicated DDR genes using RNA from cells as in A. (C) Partial restoration of DDR genes upon drug withdrawal. qRT-PCR for the indicated DDR genes in 22RV1 parental and BETi-resistant cells after drug withdrawal for 0, 4 and 12-days. (D) Lack of DNA damage upon transient treatment with JQ1 in 22Rv1 cells. 22Rv1 cells were treated with DMSO or JQ1 at the indicated concentration for 48h. COMET assays were done in the parental and BETi-resistant 22Rv1 cells and the tail moments were determined as described in the Methods section. Bars represent mean values of tail moment from two independent experiments.

Supplemental Experimental Procedures

Drugs.

JQ1 (Cayman Chemical Company -11187), I-BET762 (Cayman Chemical Company-10676), OTX-015 (Cayman Chemical Company-15947), Olaparib (Selleckchem -AZD2281), LDC000067 (Selleckchem-S7461), Dinaciclib (Selleckchem-S2768), and GSK126 (MedChem Express-HY-13470) were dissolved and aliquoted in DMSO (Sigma-Aldrich-D2650). Enzalutamide (Selleckchem-S1250) and Dihydrotestosterone was diluted and aliquoted in ethanol and Cisplatin (Sigma) was diluted in nuclease free water. Chemical synthesis and characterization of the PROTAC-BETdegrader ZBC260 and BET inhibitor HJB97 were described previously (Bai et al., 2017; Zhou et al., 2017).

Cell Culture and Development of BETi Resistant Lines.

22RV1 and LNcaP prostate cancer cells were cultured in RPMI1640 (Gibco) supplemented with 10% (v/v) FBS (Gibco). BETi (JQ1) resistant lines were developed by culturing in above mentioned media with IC50 concentration of the drug (100nM and 200nM for LNcaP and 22RV1 respectively) for over a period of 14-16 weeks. Surviving BETi resistant polyclonal pools were maintained in JQ1 throughout. All experiments for BETi resistant pools were done in presence of JQ1, except those where other BET inhibitors (ZBC260, HJB97, I-BET762 and OTX-015) were used. For starvation-stimulation of AR signalling, cells were plated in complete media at required confluency. After 24h cells were washed with DPBS and cultured in RPMI 1640 without Phenol Red (Invitrogen 11835030) with 10% charcoal-dextran stripped FBS (Gemini Bio-Products- 100119) for 72h. Starved cells were stimulated with DHT for 24 hours (unless otherwise specified).

Cell Viability Assay

Cells were plated at 5,000 per well in 96 well plate in a total volume of 100µl media with 10% FBS. Serially diluted compounds in 100 µl media were added to the cells 12 h later. After 96 h incubation, cell viability was assessed by Cell-Titer GLO (Promega). The values were normalized and IC_{50} was calculated using GraphPad Prism software.

siRNA Transfections

For siRNA mediated BRD4, AR, CDK9 and MYC knockdown experiments, cells were seeded in 10cm plates and transfected with 50 nM ON-TARGETplus SMARTpool siRNA (ThemoScientific) non-targeting control (Catalogue no. D-001810-10-50) or siRNA pools targeting the genes using Lipofectamine RNAiMax (Life Technologies 13778150). The following is the catalogue number of the siRNAs - SMARTpool: ON-TARGETplus BRD4 siRNA, (Dharmacon L-004937-00-0005), SMARTpool: ON-TARGETplus AR siRNA (Dharmacon L-003400-00-0005), SMARTpool: ON-TARGETplus MYC siRNA (Dharmacon L-003282-02-0005) and SMARTpool: ON-TARGETplus

CDK9 siRNA (Dharmacon L-003243-00-0005). Two successive transfections were carried out at an interval of 24h. Cells were harvested 48h post first transfection for western blot, qRT-PCR analysis and cell proliferation assay.

Cell proliferation assay

For cell proliferation assays after siRNA knockdown, cells were plated at 20,000 cell per well in 24-well plates (n=3) and were harvested and counted at the indicated time points by Countess™ II Automated Cell Counter (Fisher Scientific).

Colony formation assay

Cells were plated at 5,000 cells per well in 6 well plates with complete media. After 24h media was replaced with complete media containing various dilutions of the drugs and cultured for 14-20 days. Media was changed every 4-5 days. Colonies were fixed and stained using 0.5% (w/v) crystal violet (Sigma-C0775) in 20% (v/v) methanol for 30min, washed with water, and air-dried. For colorimetric assays, the stained wells were treated with 500 µl 10% acetic acid and the absorbance was measured at 590nm using a spectrophotometer.

RNA isolation and qRT-PCR assays

Total RNA was extracted using RNeasy Mini Kit (Qiagen-74106) and cDNA was synthesized from 1,000ng total RNA using SuperScriptIV (Life Technologies-18090200). qRT-PCR was performed using Fast SYBR Master Mix (Life Technologies- 4385617) or Taqman Fast Advance MMIX (Life Technologies-4444964) on QuantStudio3 (Applied Biosystems). Targets were quantified using $\Delta\Delta C_t$ method and normalized using GAPDH transcript levels. Primers were designed using Primer3 Input (version 0.4.0) (http://bioinfo.ut.ee/primer3-0.4.0/primer3/) and synthesized by Integrated DNA Technologies.

RNA-seq Library Construction and Analysis

RNA-seq libraries were constructed using the TruSeq sample Prep Kit V2 (Illumina) according to the manufacturer's instructions. Briefly, 2µg of purified RNA was poly-A selected and fragmented with fragmentation enzyme. After first and second strand synthesis from a template of poly-A selected/fragmented RNA, other procedures from end-repair to PCR amplification were done according to library construction steps. Libraries were purified and validated for appropriate size on a 2100 Bioanalyzer High Sensitivity DNA chip (Agilent Technologies, Inc.). The DNA library was quantitated using Qubit and normalized to 2nM prior to pooling. Libraries were pooled in an equimolar fashion and diluted to 10pM. Library pools were clustered and run on Nextseq500 platform with paired-end reads of 75 bases, according to the manufacturer's recommended protocol (Illumina

Inc.). Raw reads passing the Illumina RTA quality filter were pre-processed using FASTQC for sequencing base quality control.

Sequence reads were mapped to UCSC human genome build using TopHat and differential gene expression determined using Cufflinks 2.1.1 and Cuffdiff2.1.1 as implemented in BaseSpace (https://basespace.illumina.com/home/indexIllumina, San Diego CA).

Gene Set Enrichment Analysis (GSEA) was performed using the JAVA program (http://www.broadinstitute.org/gsea) as described previously (Asangani et al., 2014).

The AR target gene signature used in GSEA analysis was generated from RNAseq data with common upregulated genes in VCaP and LNCaP upon DHT treatment and the gene list is as follows:

ABCC1, ABCC4, ABHD2, ABHD3, AC002467.7, AC015871.2, AC018804.3, AC020571.3, AC058791.1, AC058791.2, AC097724.3, AC107016.1, AC126118.1, ACAA1, ACAD8, ACAT2, ACLY, ACSL3, ADM2, AFF3, AGR2, AL139819.1, ALDH1A3, ALPK3, ANK1, ANKRD37, ANXA2, AP003419.11, APIP, APPBP2, ARFGAP3, ARMC12, ARPC4-TTLL3, ASRGL1, ATP10A, ATP1A1, ATP6V0A2, AZGP1, AZGP1P1, B2M, B4GALT1, BCAR3, BHLHA15, C12orf44, C19orf10, C1orf85,C2, CACNG4, CADM2, CANT1, CAPZB, CBLL1, CCDC141, CDC14B, CDC42EP3,CDYL2, CECR6, CENPN, CHRNA2, CLDN8, CMC2, CNKSR2, CORO2A, CPSF1P1, CREB3L2, CREB3L4, CRISP3, CSGALNACT1, CTA-292E10.6, CTD-2008A1.1, CTD-2531, D15.5, DBI, DHCR24, DISP2, DNAJB9, DNAJC10, DNAJC3, EAF2, EBP, EFCAB12, ELL2, ELOVL5, EMP1, ENDOD1, EPS8L1, ERN1, ERRFI1, FADS1, FADS2, FAM129A, FAM13A-AS1, FAM13C, FAM189A2, FASN, FDFT1, FDPS, FICD, FKBP1B, FKBP5, FXYD3, FZD5, FZD8, GADD45B, GADD45G, GGT3P, GLRX2, GLUD1, GMPPB, GNB4, GNMT, GREB1, GSR, HERC3, HERPUD1, HIST1H1E, HIST1H2AD, HLA-DPA3, HMGCR, HMGCS1, HMGXB3, HOMER2, IDH1, IDI1, IGF1R, INPP4B, INSIG1, JAM3, KCNMA1, KLF15, KLF4, KLHL29, KLK2, KLK3, KLK4, KRT18, KRT19, KRT8, LAMC1, LAT2, LDLR, LDLRAD3, LIFR, LIFR-AS1, LIN7B, LINC00361, LOX, LPAR3, LRIG1, LRRFIP2, LSS, MAF, MANF, MAPK6, MBOAT2, MERTK, Metazoa_SRP, MICAL1, MIR210HG, MIR22HG, MLPH, MOGAT2, MPC2, MSMO1, MTMR9, MTOR, MVD, MVK, MYBPC1, MYOF, NAT1, NBL1, NCAPD3, NDFIP2, NDRG1, NNMT, ODC1, OR7E5P, ORM1, ORM2, PART1, PCDH1, PCYT2,PDIA5, PER1, PEX10, PFKFB2, PGC, PGM3, PHLDA2, PPAPDC2, PPP1CB, PTPRM, RAB27A, RAB3B, RAB4B, RASD1, RHOU, RP11-109D20.2, RP11-1100L3.8, RP11-175B9.3, RP1-117B12.4, RP11-18F14.2, RP11-191G24.1, RP11-244F12.3, RP11-314O13.1, RP11-326A19.5, RP11-443A13.3, RP11-456A18.1, RP11-66B24.4, RP11-67L3.5, RP13-15M17.1, RP13-650J16.1, RP1-90G24.10, RP4-539M6.19, RPL32P29, RPLP1P11, S100P, SASH1, SAT1, SCD, SDF2L1, SDK1, SEC14L2, SEC24D, SEPP1, SGK1, SHROOM3, SLC15A2, SLC16A3, SLC16A6, SLC1A5, SLC25A20, SLC2A3, SLC41A1, SLC43A1, SLC45A3, SMPD2, SMS, SNAI2, SNCG, SNX25, SOCS2, SOCS2-AS1, SORD, SPATA6L, SPCS3, SPDEF, SPOCK1, SPTB, SQLE, SSR3, ST6GALNAC1, STARD4, STEAP4, STK17B, STK39, STK40, STYK1, SWT1, TBX15, TECPR1, TGM2, THSD7A, TIPARP, TMCC3, TMED9, TMEM79, TMEM87B, TMPRSS2, TPD52, TRIM36, TRPM8, TTN, TUBA3D,TUBA3E,U3, VPS26B, WIPI1, WWC1, XBP1, ZBED3-AS1, ZBTB16, ZDHHC8P1, ZFP36.

The RNA-seq data can be found at the Gene Expression Omnibus under accession # GSE103082.

Protein Extraction and Immunoblot Analysis

Total protein was extracted using RIPA buffer (Boston BioProducts BP-115DG) containing Pierce protease inhibitor (Life Technologies-88266) and Halt protease & phosphatase Inhibitors (Life Technologies-78443). Lysates were sonicated and spun at 13,000rpm for 15min to remove debris. For nuclear and cytoplasmic protein extraction, NE-PER™ Nuclear and Cytoplasmic Extraction Reagents (Thermo Scientific-78835) was used, following manufacturer's instructions. Proteins were quantified using BCA Protein assay (Life Technologies-23250), normalised and samples of 2µg/µl were made using Laemmli Sample Buffer (Bio-Rad-1610737) and boiled (95˚C, 10min). 15-20µg samples were run on polyacrylamide gels (Bio-Rad-1610173) using Sub Cell GT System (Bio-Rad- 1704486) and transferred using TurboBlot (Bio-Rad-1704150) to polyvinylidene difluoride (PVDF) membrane (EMD Millipore-IPVH00010). The membranes were blocked for 1h in 5% (w/v) milk in Tris-buffered Saline with 0.1% (v/v) Tween (TBS-T) and incubated overnight at 4˚C with the primary antibody in 5%milk. Membranes were washed multiple times before being incubated for 1h with Peroxidase conjugated secondary antibody in 5% milk and signals were visualized using SuperSignal Femto (Life Technologies Corporation-34096) as per manufacturer's protocol. Antibodies used in the study are shown in Table S2.

Protein Stability

Cells (at 50% confluency) were treated with 20µg/µl cycloheximide for various time intervals (0h, 3h, 6h, 12h, 24h, and 36h). Proteins were extracts as described above followed by immunoblot analysis.

Chromatin–bound Protein Extraction

Chromatin bound protein extraction was adapted from the protocol described previously (Sankaran et al., 2016) . Briefly, 10 X 10^6 were collected and washed with DPBS. Cells were resuspended in 250µl Buffer A (10mM HEPES pH 7.9, 10 mM KCl, 1.5mM MgCl2, 0.34M sucrose, 10% glycerol, 1mM DTT) supplemented with 0.1% TritonX-100, and incubated on ice for 10min. Nuclei pellet was collected by centrifuging at 1300 x *g* for 5min at 4˚C, washed in Buffer A and centrifuged again. Nuclei pellet was then resuspended in Buffer B (3mM EDTA, 0.2mM EGTA, 1mM DTT) and incubated on ice for 30 min. Chromatin pellet was collected by centrifuging at 1700 x *g* for 5min at 4˚C, washed in Buffer B and centrifuged again. The proteins were incubated on ice in Buffer B with 150mM NaCl for 20min and centrifuged at 1700 x *g* for 5 mins to remove proteins soluble in 150mM salt concentrations. Pellet was then incubated in Buffer B with 300mM NaCl on ice for 20min and centrifuged again at 1700 x *g* to get final chromatin pellet. The chromatin pellet was dissolved in sample buffer, sonicated for 15s, and boiled at 95˚C for 10 mins. Samples were analysed using Immunoblot analysis mentioned above. All buffers were supplemented with Pierce protease inhibitor and Halt protease & phosphatase Inhibitors.

Dot Blot

Proteins were diluted to a concentration of 2µg/µl, 1-2µl of the protein was applied to PVDF membrane (EMD Millipore-IPVH00010) and allowed to be absorbed for 5min. The membranes were blotted with specific antibodies and processed as in immunoblot procedure.

Cellular Thermal Shift Assay (CETSA)

Cells were treated with DMSO or JQ1 for 3h, trypsinised, counted and aliquoted in PBS (with protease inhibitors). Cells were heated at indicated temperatures for 3min in thermal cycler followed by cooling at RT for 3min. cells were lysed by 2 freeze-thaw cycles followed by centrifugation at 20,000g for 20min at 4˚C. Supernatants were collected and analysed by immunoblotting.

Immunofluorescence

75,000 cells per well were seeded on coverslips placed in 24-well plates in media with 10% FBS. After 48h, media was removed and washed with PBS (Ca^{2+}, Mg^{2+} free). Cells were fixed with 3% paraformaldehyde for 10 min at room temperature, washed twice with PBS and permeabilized with PBS/0.5% Triton-X 100 for 10min at 40˚C followed by washing twice with PBST. Primary antibody diluted in PBST was added to the coverslips and incubated in a humidified chamber at 37˚C for 20min. Cover slips containing cells were washed 3 times with PBST. Alexa fluor secondary antibody diluted (1:200) in PBST was added to the coverslips and incubated in a humidified chamber at 37˚C for 20 min. The cover clips were washed four times with PBST before mounting on onto glass slides using Vectashield mounting medium containing DAPI (Vector Laboratories). Multiple images were captured from different fields using fluorescence microscope.

Comet Assay

Cells were trypsinized and resuspended in PBS (Ca^{2+}, Mg^{2+} free) at a density of $1X10^5$/ml. Cells were mixed with molten LM Agarose at a ratio of 1:10 (v/v) and immediately pipetted 50µl onto Comet Slide and spread evenly (Trivigen Inc.). Slides were placed flat at 4˚C in the dark for 30min. Slides were immersed in 4˚C lysis solution and incubated overnight at 4˚C. Excess buffer was drained from slides and immersed in freshly prepared alkaline unwinding solution and kept at 4˚C for 1 h. Slides were placed in electrophoresis unit and run at 16V for 40min. Excess buffer was drained out and slides were immersed twice in water for 5min each and then in 70% ethanol for 5 min. Samples were dried at 37˚C for 15min. Slides were stained with SYBR Gold (Fisher Scientific S11494) for 30min and briefly rinsed in water. Slides were dried at 37˚C and observed under fluorescent microscope (EVOS).

Cell Cycle Analysis

For cell cycle analysis, BETi resistant cells and their respective parental control cells grown in 6-well plates were washed with PBS and fixed in 70% ethanol overnight. The cells were washed again with PBS, stained with propidium iodide and analysed by flow cytometry**.**

Chromatin Immunoprecipitation (ChIP) and ChIP-seq.

The ChIP assay for BRD4, H3K27acetyl H3K27me3 and gH2A.x were performed with respective antibody (Table S2) using HighCell ChIP kit (Diagenode) according to the manufacturer's protocol. IgG was used as a negative control in all ChIP reaction. Briefly, cells were crosslinked for 10min with 1% (v/v) formaldehyde. Crosslinking was terminated by the addition of 1/10 volume 1.25M glycine for 5min at room temperature followed by cell lysis and sonication (Bioruptor, Diagenode), resulting in an average chromatin fragment size of 200 bp. Chromatin equivalent to $10x10^6$ cells were used for ChIP using various antibodies. ChIP DNA was isolated (IPure Kit, Diagenode) from samples by incubation with the antibody at 4˚C overnight followed by washing and reversal of crosslinking. The eluted DNA was used for qPCR using appropriate primers as previously described (Asangani et al., 2014). The primer sequences used for ChIP-qPCR are provided in Table S2.

ChIP-seq was done for BRD4, H3K27ac and IgG contorl in LNCaP cells. The ChIP-seq sample preparation for sequencing was performed according to the manufacturer's instructions (Illumina). ChIP-enriched DNA samples (1–10 ng) were converted to blunt ended fragments using T4 DNA polymerase, *E. coli* DNA polymerase I large fragment (Klenow polymerase) and T4 polynuleotide kinase (New England BioLabs (NEB)). A single A base was added to fragment ends by Klenow fragment (3' to 5' exo minus; NEB) followed by ligation of Illumina adaptors (Quick ligase, NEB). The adaptor modified DNA fragments were enriched by PCR using the Illumina Barcode primers and Phusion DNA polymerase (NEB). PCR products were size selected using 3% NuSieve agarose gels (Lonza) followed by gel extraction using QIAEX II reagents (Qiagen). Libraries were quantified with the Bioanalyzer 2100 (Agilent) and sequenced on the Illumina HiSeq 2000 Sequencer (100-nucleotide read length).

The ChIP-seq reads were aligned to the HG19 reference using Bowtie2 (Subramanian et al., 2005) with all default settings. Duplicate fragments (based on the coordinates of both reads) and fragments with only one mapped read were removed using samtools (Li et al., 2009). To correct for differences in sequencing depth and alignment coverage the values were further normalized by the number of aligned reads per million. ChIP-seq signals were visualized in the UCSC genome browser by converting the BedGraph files into BigWig files using bedGraphtoBigWig (Kent et al., 2010).

Table S2: Primer sequences for SYBR green PCR, Alu primer probe for TaqMan PCR and antibodies used in the study. (Related to Experimental Procedures)

Gene	Forward Primer	Reverse Primer
AR	CAGTGGATGGGCTGAAAAAT	GGAGCTTGGTGAGCTGGTAG
AR-V7	CCATCTTGTCGTCTTCGGAAATGTTA	TTTGAATGAGGCAAGTCAGCCTTTCT
KLK3	ACGCTGGACAGGGGGCAAAAG	GGGCAGGGCACATGGTTCACT
TMPRSS2	CAGGAGTGTACGGGAATGTGATGGT	GATTAGCCGTCTGCCCTCATTTGT
FKBP5	TCTCATGTCTCCCCAGTTCC	TTCTGGCTTTCACGTCTGTG
SLC45A3	TCGTGGGCGAGGGGCTGTA	CATCCGAACGCCTTCATCATAGTGT
BMPR1B	GTCCTGGACCCAGTTGTACCT	TCTAGGGTGGTGGACTTCAGA
ZBTB16	CAGTTTTCGAAGGAGGATGC	CCCACACAGCAGACAGAAGA
ATM	CCAGCAGACCAGCCAATTAC	TTCTCCTGTGTGGTCCACCT
ATR	AGGAGCCTATCCTGGCTCTC	TAGCTACCCTGGCACTCTGC
PALB2	GAAGCCCTGTGTTTCAGCTC	ACCCGACCATTTCACAAAAG
PARP1	GTCCCAGGGTCTTCGGATAG	CCCTGAGACGTATGGCAGTAG
CHEK1	TGTCAGAGTCTCCCAGTGGA	GGTTCTGGCTGAGAACTGGA
CHEK2	CACAGCTCTACCCCAGGTTCT	CACAACACAGCAGCACACAC
BRCA1	AGCTGTGTGGTGCTTCTGTG	GAAGCCATTGTCCTCTGTCC
BRCA2	GAGCCCCTTCACTTCAGCAA	TAGACGAAAGGGGCAAGTCC
RAD51	GGTGAAGGAAAGGCCATGTA	CATCACTGCCAGAGAGACCA
MDC1	GAATGACAACTGGGGTTGCT	CTCAGCCTTTTGGCTTCATC
GAPDH	TGCACCACCAACTGCTTAGC	GGCATGGACTGTGGTCATGAG
ChIP-PCR BRCA1	TAGGTAGCGATTCTGACCTTCG	GCCCTCTAGCCTCTACTCTTCC
ChIP-PCR BRCA2	CCGCTTTATTCGGTCAGATACT	CTGCGGGTATTTCTCAGTGTG
ChIP-PCR MDC1	TGTCTAGGAGGACCGAGGAA	GAGGGGCTGTGTCATAGACG
ChIP-PCR CHEK1	GCAGCTGCTGCTGGTTTCTC	ACAGTCGGTGAAGCAGAGTG
ChIP-PCR CHEK2	ATCTAGCCGTGGTCACTCGT	CCAGCCAATCAGCAACATTA
ChIP-PCR PALB2	AGGGTTGGAAAGAGGAGGATAC	CGAGCTGCTCTACAACAAGTCT
ChIP-PCR RAD51	GAGGGACTGGGGTAGGAGTAG	GAGGCGAGAGTATCGTCTGAG
ChIP-PCR ERG	TTTCTGGCTGTTTGCTGAAAT	CCGACCAAGTGAAAACTACCC
Human Alu	GTCAGGAGATCGAGACCATCCT	AGTGGCGCAATCTCGGC
Human Alu TaqMan probe	6-FAM-AGCTACTCGGGAGGCTGAGGCAGGA-TAMRA	
	Antibodies used in the study	

Antibody	Application	Source	Catalogue No.
Anti-BRD4	IB/ ChIP / ChIP-seq	Bethyl Laboratories	A301-985A50
Anti-BRD3	IB	Santa Cruz Biotechnology	SC-81202
Anti-BRD2	IB	Abnova	PAB3245
Anti-c-Myc	IB	Abcam Inc.	ab32072
Anti-pS81-AR	IB/IF	EMD Millipore	07-1375-EMD
Anti-AR	IB	EMD Millipore	06-680-EMD
Anti-EZH2	IB	BD Transduction Laboratories	BDB612667
Anti-CDK9	IB	Cell Signaling Technology	2316S
Anti-PSA	IB	Daco North America	A0562
Anti-γH2A.X (Ser139/Tyr142)	IB/IF/ChIP	Cell Signaling Technology	5438S
Anti-H2A.X	IB	Cell Signaling Technology	2595S
Anti-H3K27me3	IB	Cell Signaling Technology	9733S
Anti-H3K36me3	IB	Abcam Inc.	ab9050
Anti-H3K27ac	IB/ChIP/ChIP-seq	Active Motif	39133

Anti-H3K27me3	ChIP	EMD Millipore	07-449-EMD
Anti-H3	IB	Cell Signaling Technology	9715S
Anti-53BP1	IB/IF	Novus Biologicals	NB100-904
Anti-PAR	IB	GeneTex	GTX75054
Anti-cl. PARP (Asp214)	IB	Cell Signaling Technology	9541S
Anti-GAPDH	IB	Cell Signaling Technology	3683S
Anti-Mouse(peroxidase conj.)	IB	Thermo Fisher Scientific	0032430
Anti-Rabbit(peroxidase conj.)	IB	Thermo Fisher Scientific	0032460
Anti-Rabbit IgG (Alexa Fluor 568)	IF	Fisher Scientific	A-11011
Anti-Mouse IgG (Alexa Fluor 488)	IF	Fisher Scientific	A-11029

Supplemental References

Asangani, I. A., Dommeti, V. L., Wang, X., Malik, R., Cieslik, M., Yang, R., Escara-Wilke, J., Wilder-Romans, K., Dhanireddy, S., Engelke, C., *et al.* (2014). Therapeutic targeting of BET bromodomain proteins in castration-resistant prostate cancer. Nature *510*, 278-282.

Bai, L., Zhou, B., Yang, C. Y., Ji, J., McEachern, D., Przybranowski, S., Jiang, H., Hu, J., Xu, F., Zhao, Y., *et al.* (2017). Targeted Degradation of BET Proteins in Triple-Negative Breast Cancer. Cancer Res *77*, 2476-2487.

Kent, W. J., Zweig, A. S., Barber, G., Hinrichs, A. S., and Karolchik, D. (2010). BigWig and BigBed: enabling browsing of large distributed datasets. Bioinformatics *26*, 2204-2207.

Li, H., Handsaker, B., Wysoker, A., Fennell, T., Ruan, J., Homer, N., Marth, G., Abecasis, G., Durbin, R., and Genome Project Data Processing, S. (2009). The Sequence Alignment/Map format and SAMtools. Bioinformatics *25*, 2078-2079.

Sankaran, S. M., Wilkinson, A. W., Elias, J. E., and Gozani, O. (2016). A PWWP Domain of Histone-Lysine N-Methyltransferase NSD2 Binds to Dimethylated Lys-36 of Histone H3 and Regulates NSD2 Function at Chromatin. J Biol Chem *291*, 8465-8474.

Subramanian, A., Tamayo, P., Mootha, V. K., Mukherjee, S., Ebert, B. L., Gillette, M. A., Paulovich, A., Pomeroy, S. L., Golub, T. R., Lander, E. S., and Mesirov, J. P. (2005). Gene set enrichment analysis: a knowledge-based approach for interpreting genome-wide expression profiles. Proc Natl Acad Sci U S A *102*, 15545-15550.

Zhou, B., Hu, J., Xu, F., Chen, Z., Bai, L., Fernandez-Salas, E., Lin, M., Liu, L., Yang, C. Y., Zhao, Y., *et al.* (2017). Discovery of a Small-Molecule Degrader of Bromodomain and Extra-Terminal (BET) Proteins with Picomolar Cellular Potencies and Capable of Achieving Tumor Regression. J Med Chem.